Lipid Bilayer Environments Control Exchange Kinetics of Deep Cavitand Hosts and Enhance Disfavored Guest Conformations

Lizeth Perez, Bethany G. Caulkins, Magi Mettry, Leonard J. Mueller and Richard J. Hooley*

Department of Chemistry, University of California-Riverside, Riverside, CA 92521, United States

richard.hooley@ucr.edu

Electronic Supplementary Information

Table of Contents

1. NMR Spectra of New Compounds

Guest 3

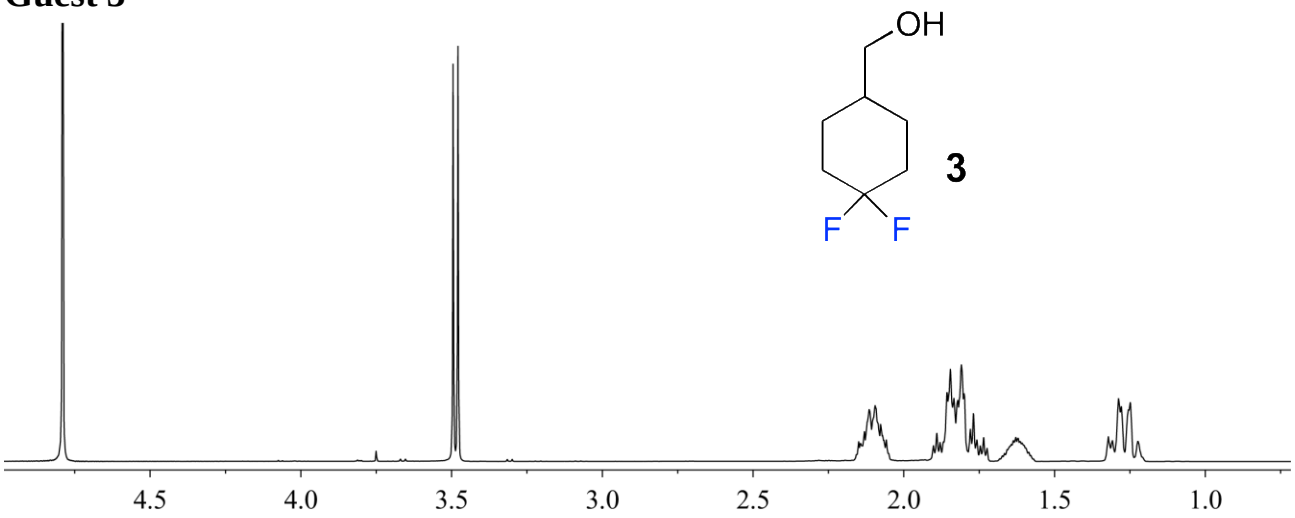

Figure S-1. ^{1}H NMR spectrum of 4,4-difluorocyclohexanemethanol guest **3** (400.13 MHz, D_2O, 298 K).

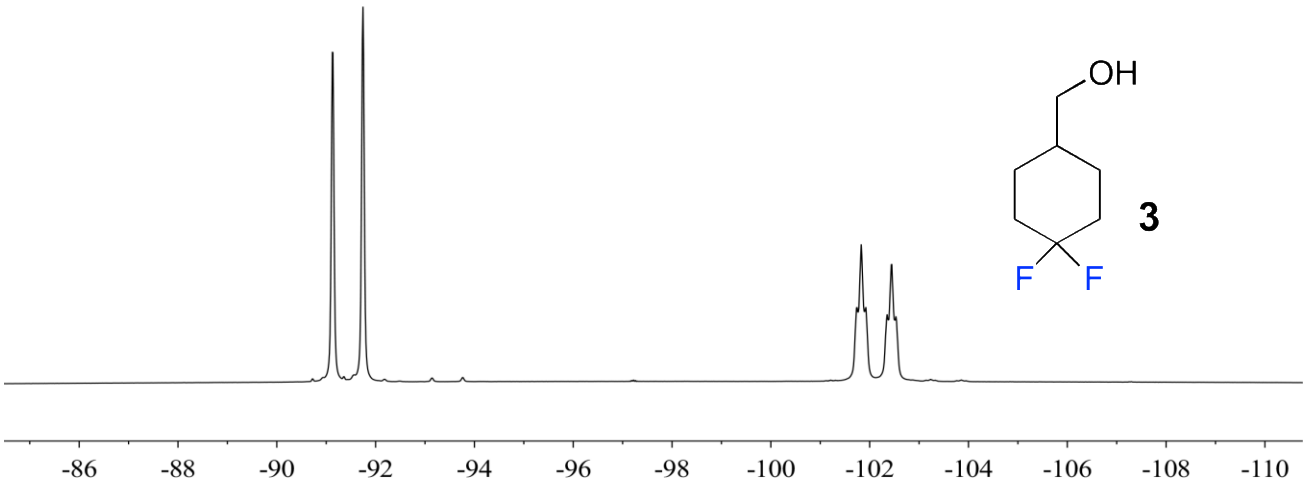

Figure S-2. ^{19}F NMR spectrum of 4,4-difluorocyclohexanemethanol guest **3** (376.50 MHz, D_2O, 298 K).

Guest 4

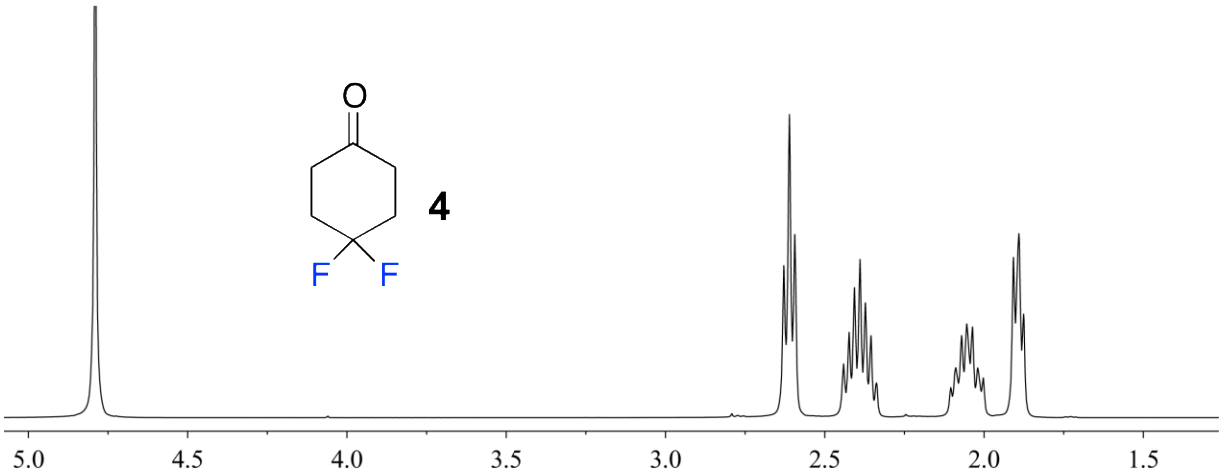

Figure S-3. ^{1}H NMR spectrum of 4,4-difluorocyclohexanone guest **4** (400.13 MHz, D_2O, 298 K).

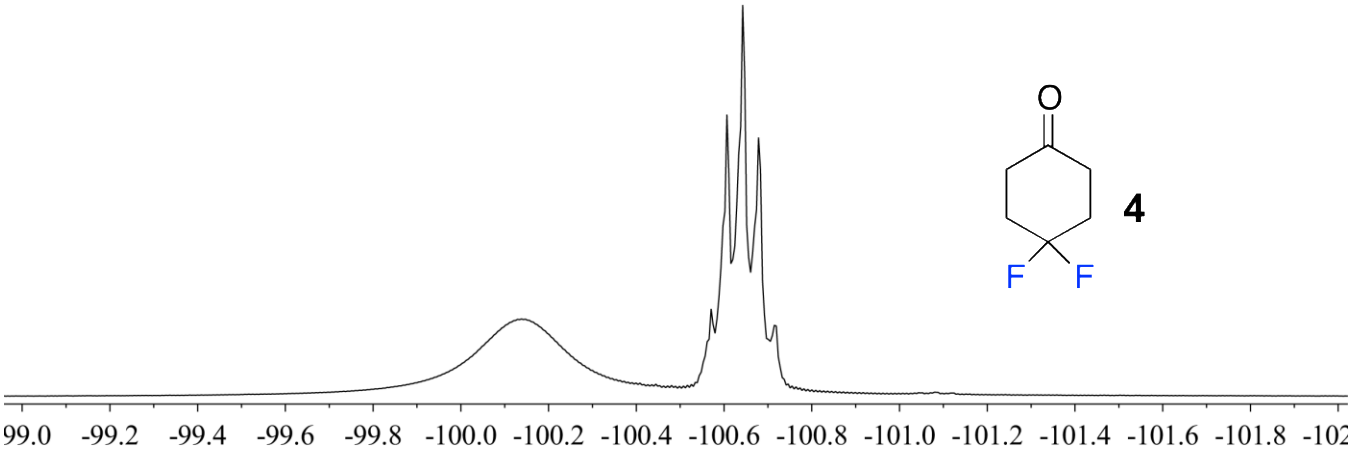

Figure S-4. ^{19}F NMR spectrum of 4,4-difluorocyclohexanone guest **4** (376.50 MHz, D_2O, 298 K).

Guest 5

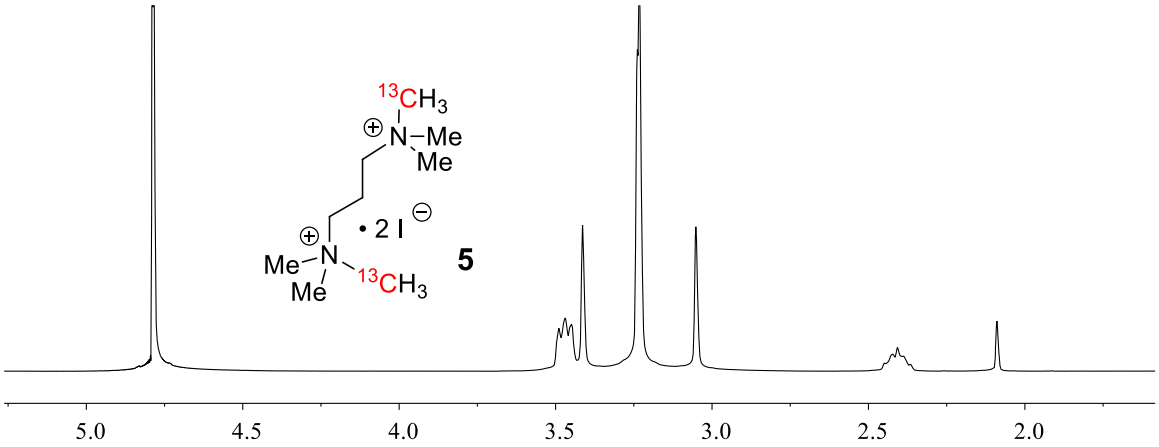

Figure S-5. ^{1}H NMR spectrum of N,N,N,N',N',N'-hexamethyl-1,3-propanediaminium diiodide-^{13}C guest **5** (400.13 MHz, D_2O, 298 K).

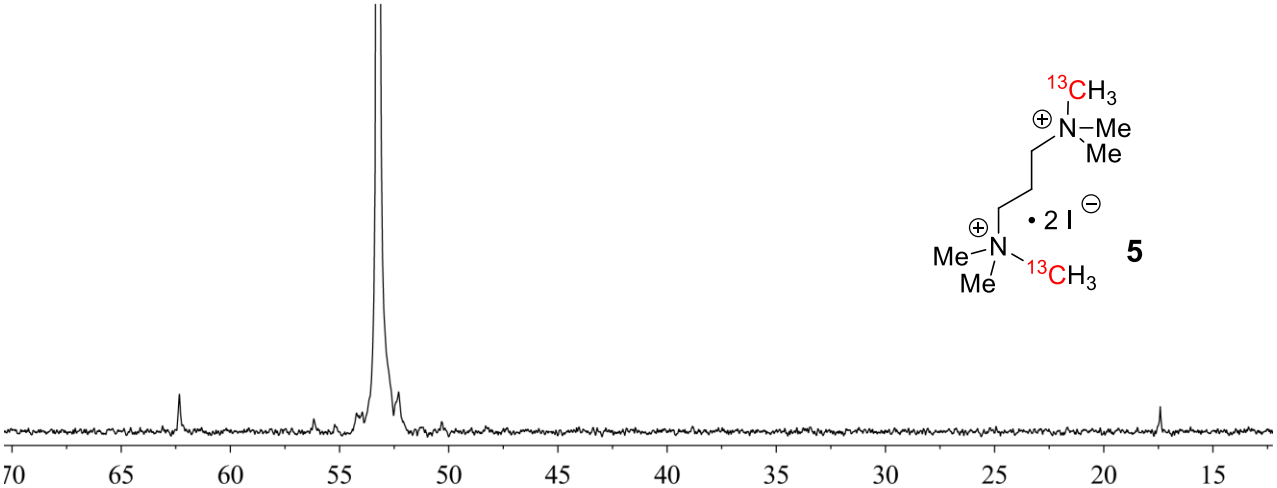

Figure S-6. ^{13}C NMR spectrum of N,N,N,N',N',N'-hexamethyl-1,3-propanediaminium diiodide-^{13}C guest **9** (100.61 MHz, D_2O, 298 K).

Guest 6

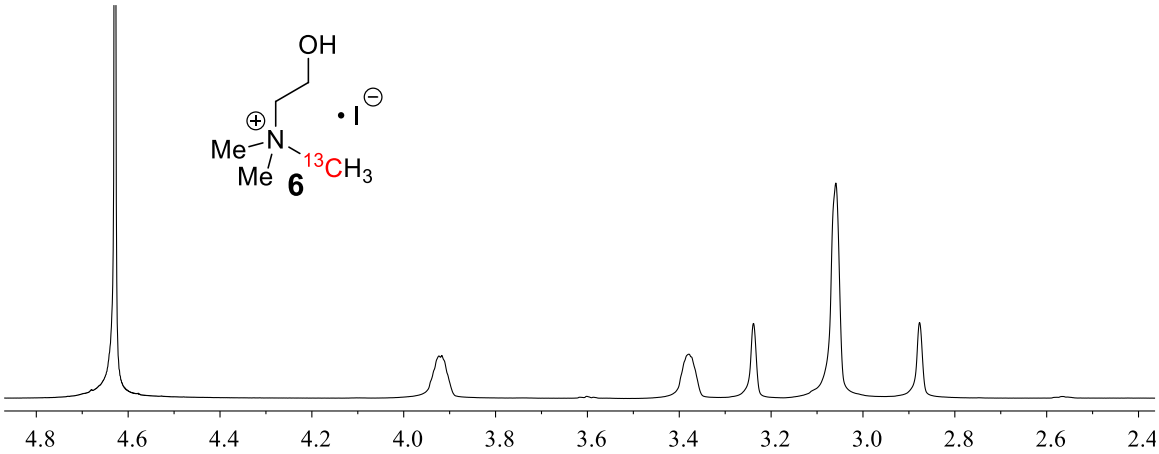

Figure S-7. ^{1}H NMR spectrum of choline iodide-^{13}C guest **6** (400.13 MHz, D_2O, 298 K).

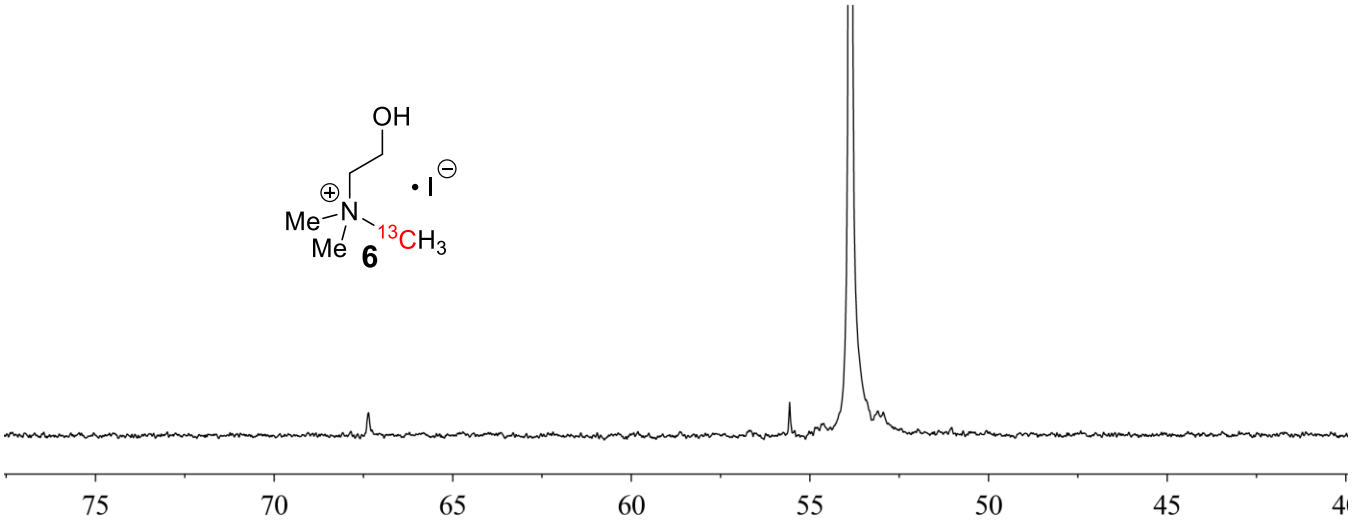

Figure S-8. ^{13}C NMR spectrum of choline iodide-^{13}C guest **6** (100.61 MHz, D_2O, 298 K).

Guest 7

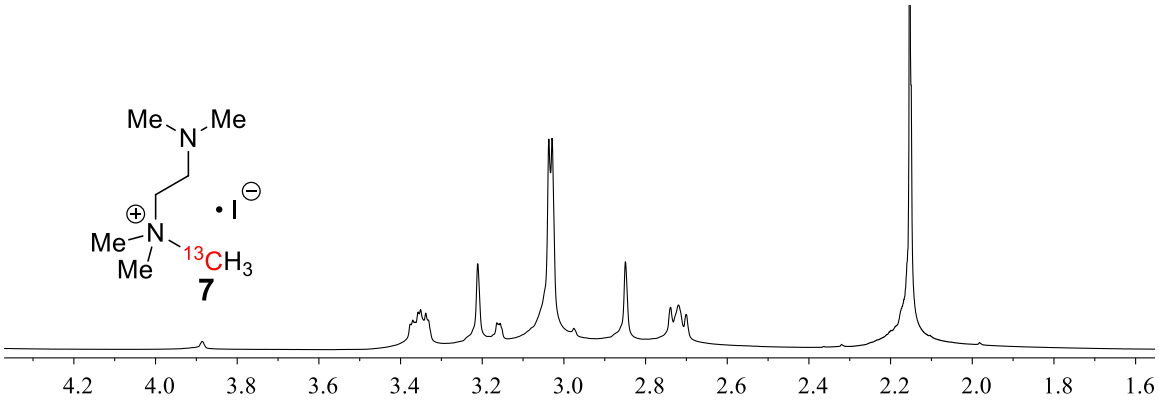

Figure S-9. ^{1}H NMR spectrum of N,N,N,N',N'-pentamethyl-1,2-ethanediaminium iodide-^{13}C guest **7** (400.13 MHz, D_2O, 298 K).

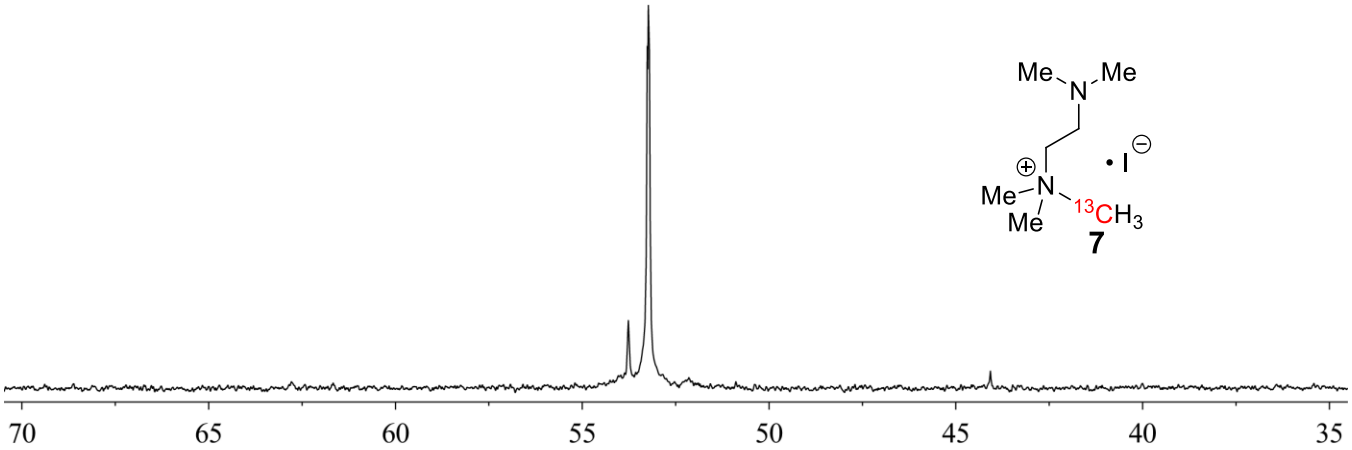

Figure S-10. ^{13}C NMR spectrum of N, N, N, N', N'-pentamethyl-1,2-ethanediaminium iodide-^{13}C guest **7** (100.61 MHz, D_2O, 298 K).

Guest 8

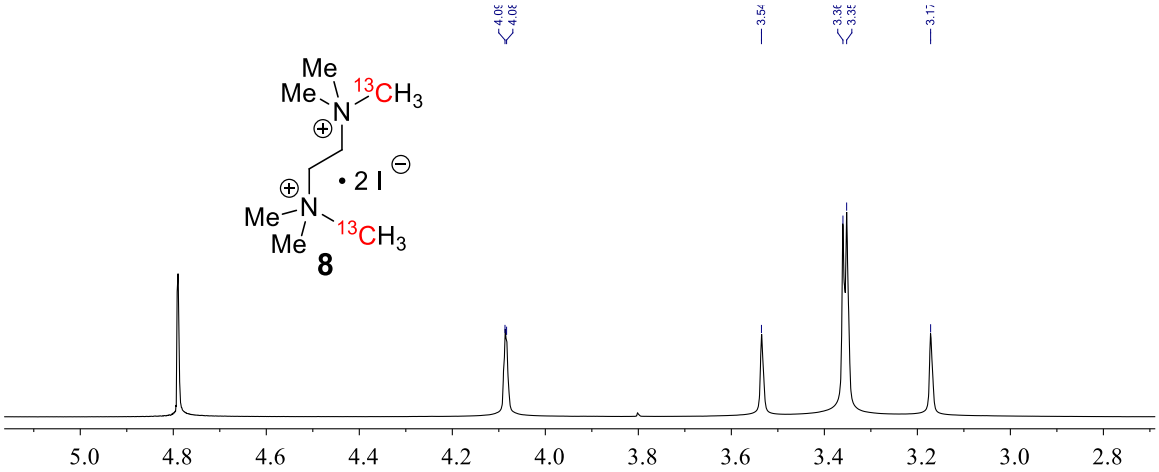

Figure S-11. ^{1}H NMR spectrum of N,N,N,N',N',N'-hexamethyl-1,2-ethanediaminium diiodide-^{13}C guest **8** (400.13 MHz, D_2O, 298 K).

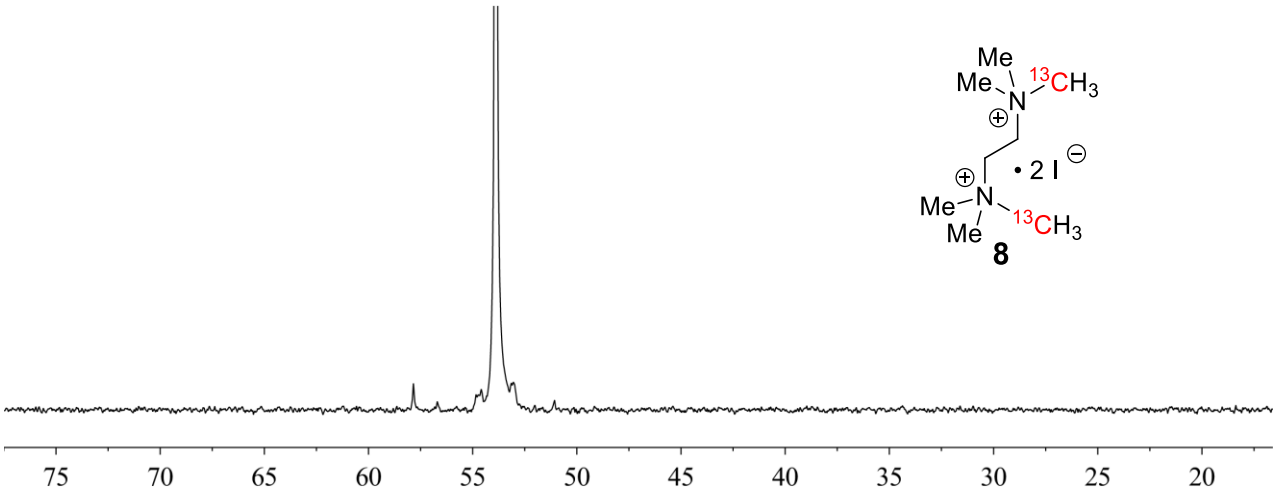

Figure S-12. ^{13}C NMR spectrum of N,N,N,N',N',N'-hexamethyl-1,2-ethanediaminium diiodide-^{13}C guest **8** (100.61 MHz, D_2O, 298 K).

2. NMR Spectra of Host:Guest Complexes in Free Aqueous Solution

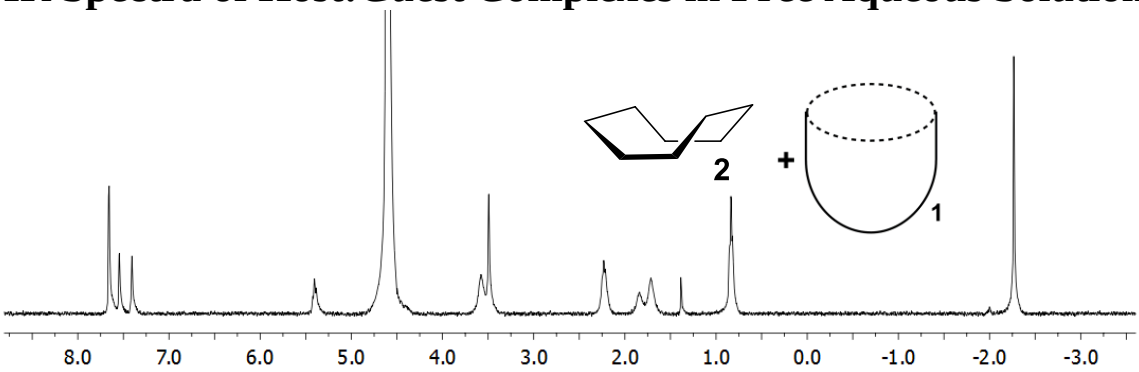

Figure S-13. ^{1}H NMR spectrum of the **1•2** cavitand-cyclooctane complex (400.13 MHz, D_2O, 298 K, [**1**] = [**2**] = 1.8 mM).

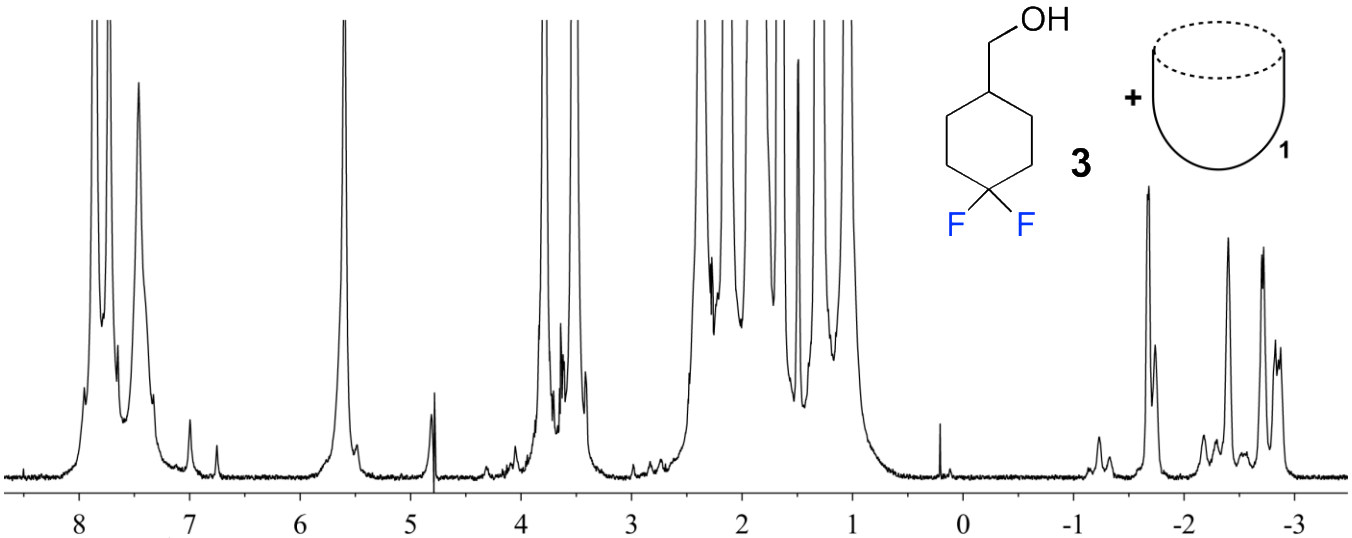

Figure S-14. ^{1}H NMR spectrum of the **1•3** cavitand-guest **3** complex (400.13 MHz, D_2O, 298 K, [**1**] = 5.8 mM, [**3**] = 39.5 mM).

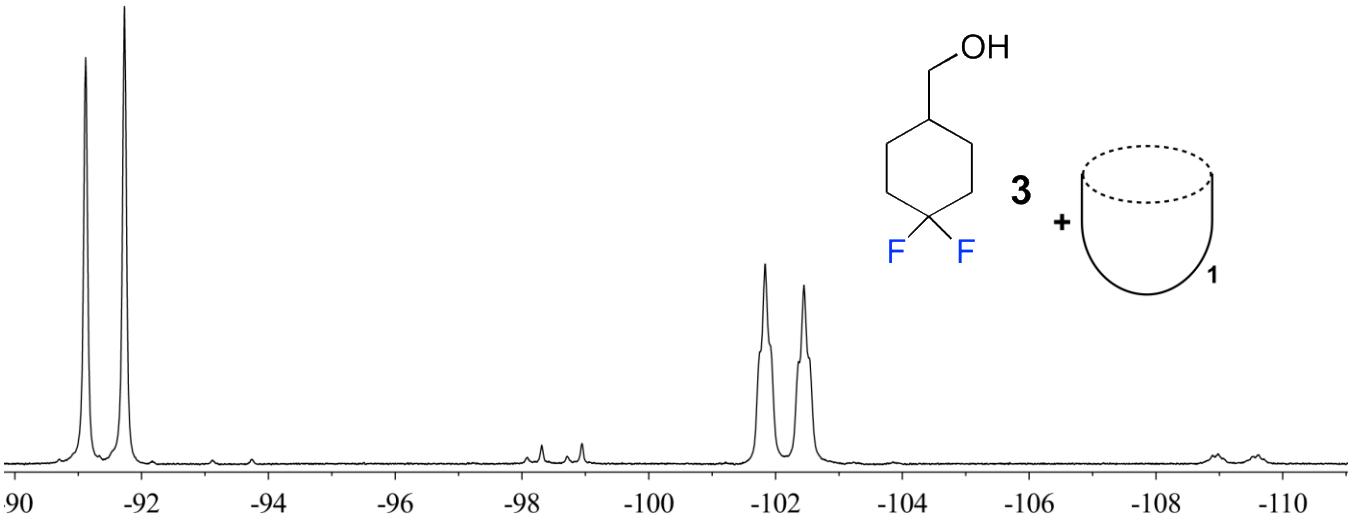

Figure S-15. ^{19}F NMR spectrum of the **1•3** cavitand-guest **3** complex (376.50 MHz, D_2O, 298 K, [**1**] = 5.8 mM, [**3**] = 39.5 mM).

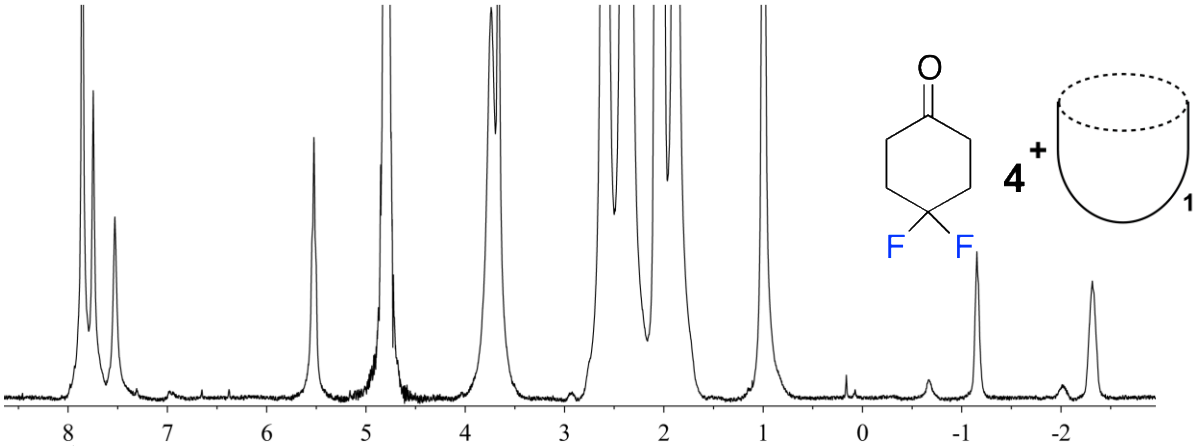

Figure S-16. ^{1}H NMR spectrum of the **1•4** cavitand-guest **4** complex (400.13 MHz, D_2O, 298 K, [**1**] = 5.8 mM, [**4**] = 39.5 mM).

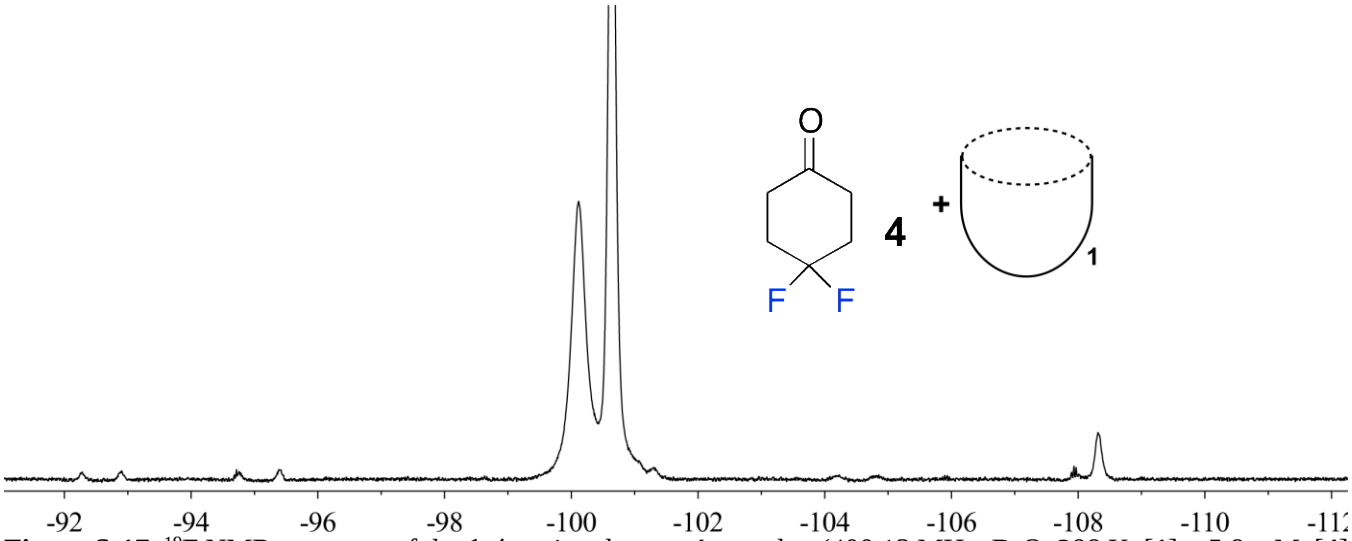

Figure S-17. ^{19}F NMR spectrum of the **1•4** cavitand-guest **4** complex (400.13 MHz, D_2O, 298 K, [**1**] = 5.8 mM, [**4**] = 39.5 mM).

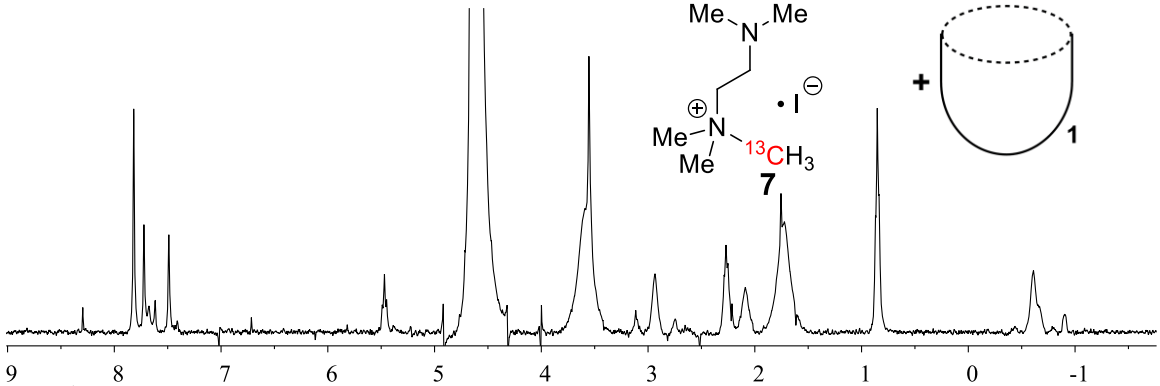

Figure S-18. ^{1}H NMR spectrum of the **1•7** cavitand-guest **7** complex (400.13 MHz, D_2O, 298 K, [**1**] = 1.8 mM, [**7**] = 2.2 mM).

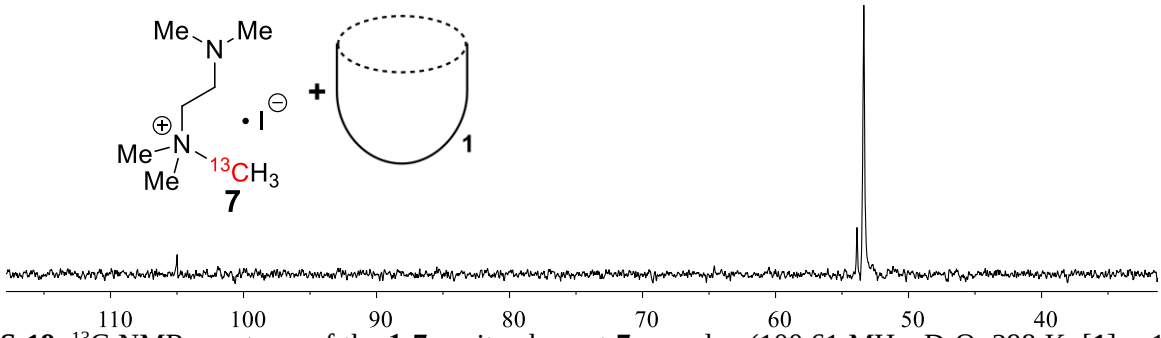

Figure S-19. ^{13}C NMR spectrum of the **1•7** cavitand-guest **7** complex (100.61 MHz, D_2O, 298 K, [**1**] = 1.8 mM, [**7**] = 2.2 mM).

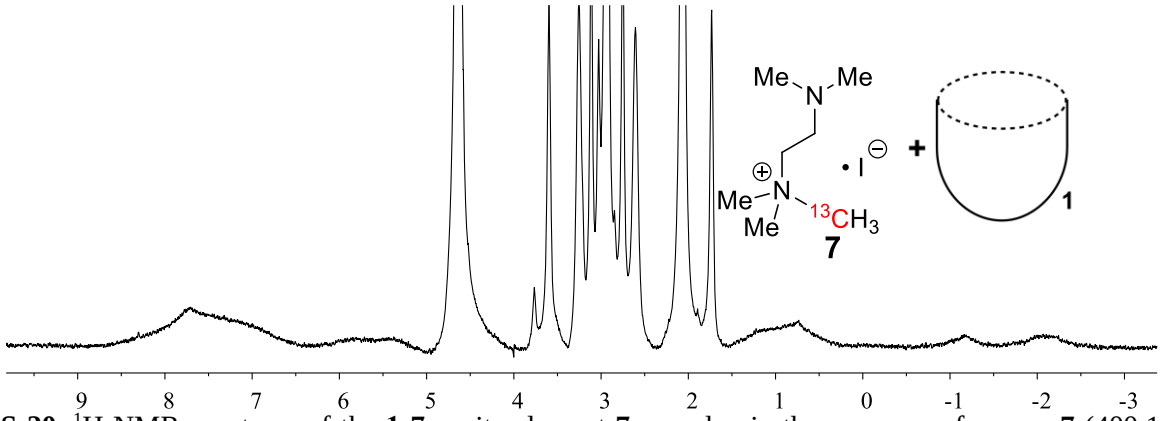

Figure S-20. ^{1}H NMR spectrum of the **1•7** cavitand-guest **7** complex in the presence of excess **7** (400.13 MHz, D_2O, 298 K, [**1**] = 1.8 mM, [**7**] = 10 mM).

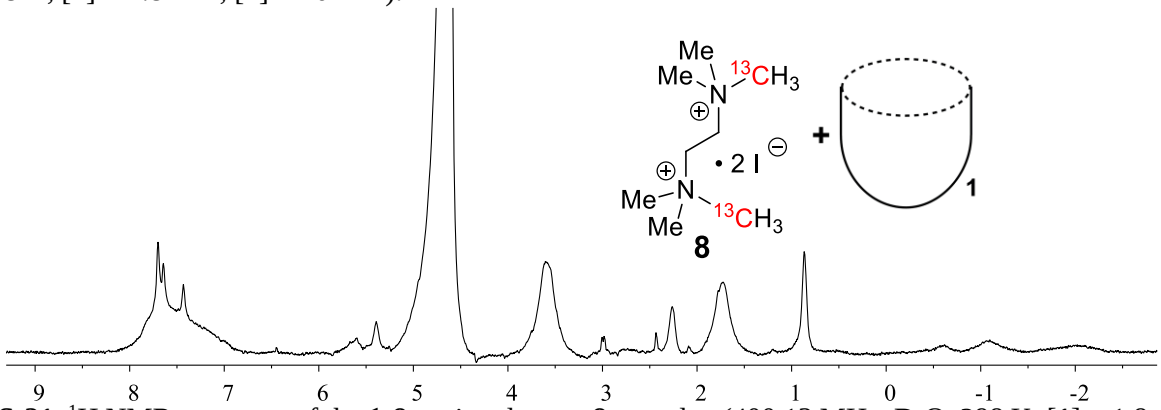

Figure S-21. ^{1}H NMR spectrum of the **1•8** cavitand-guest **8** complex (400.13 MHz, D_2O, 298 K, [**1**] = 1.8 mM, [**8**] = 2.2 mM).

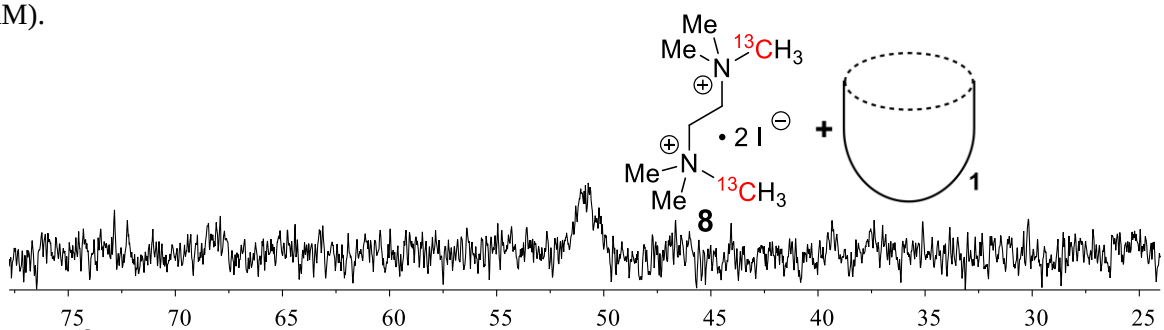

Figure S-22. ^{13}C NMR spectrum of the **1•8** cavitand-guest **8** complex (100.61 MHz, D_2O, 298 K, [**1**] = 1.8 mM, [**8**] = 2.2 mM).

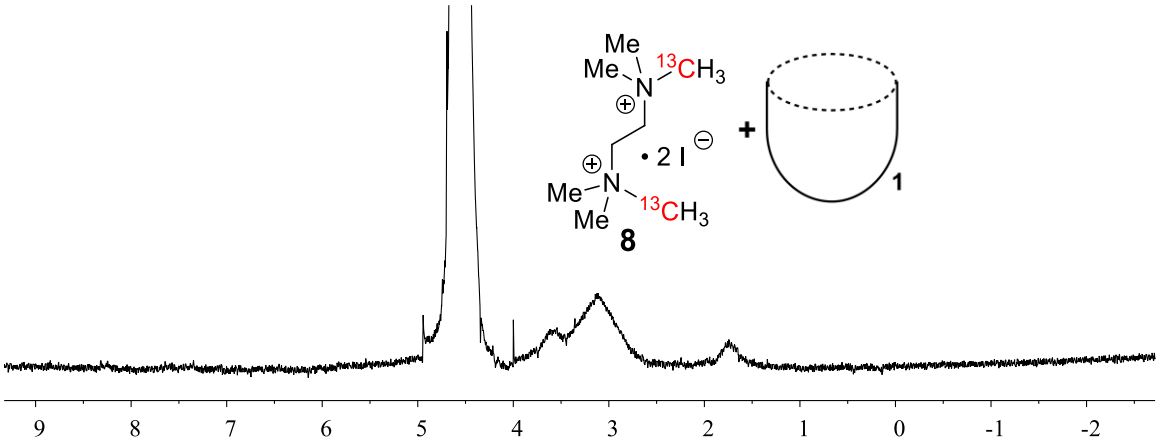

Figure S-23. ^{1}H NMR spectrum of the **1•8** cavitand-guest **8** complex in the presence of excess **8** (400.13 MHz, D_2O, 298 K, [**1**] = 1.8 mM, [**8**] = 5.5 mM).

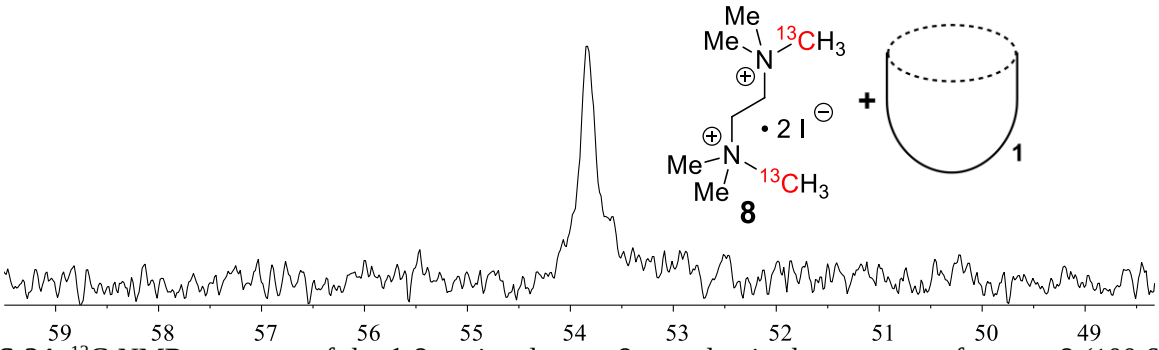

Figure S-24. ^{13}C NMR spectrum of the **1•8** cavitand-guest **8** complex in the presence of excess **8** (100.61 MHz, D_2O, 298 K, [**1**] = 1.8 mM, [**8**] = 5.5 mM).

3. NMR Spectra of Host:Guest Complexes in DMPC/DHPC Lipid Micelles.

Guest 2

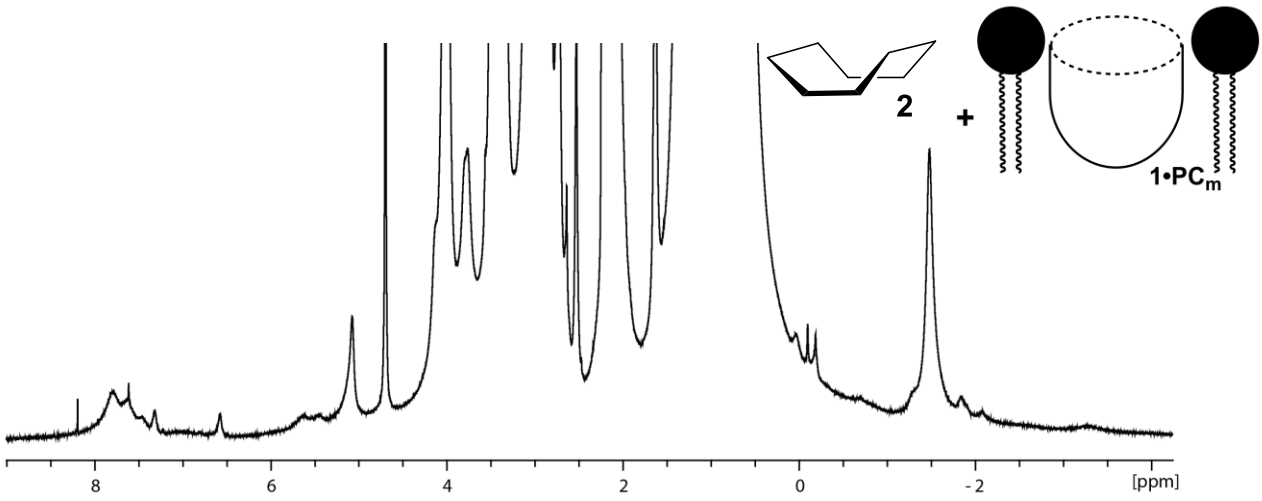

Figure S-25. ^{1}H NMR spectrum of the **1•2** cavitand-cyclooctane complex in DMPC:DHPC lipid micelles (599.88 MHz, 1 mM HEPES/D_2O, 298 K, [**1**] = [**2**] = 1.8 mM, ratio DMPC/DHPC = 3.2:1, 60 mg/mL total lipid concentration).

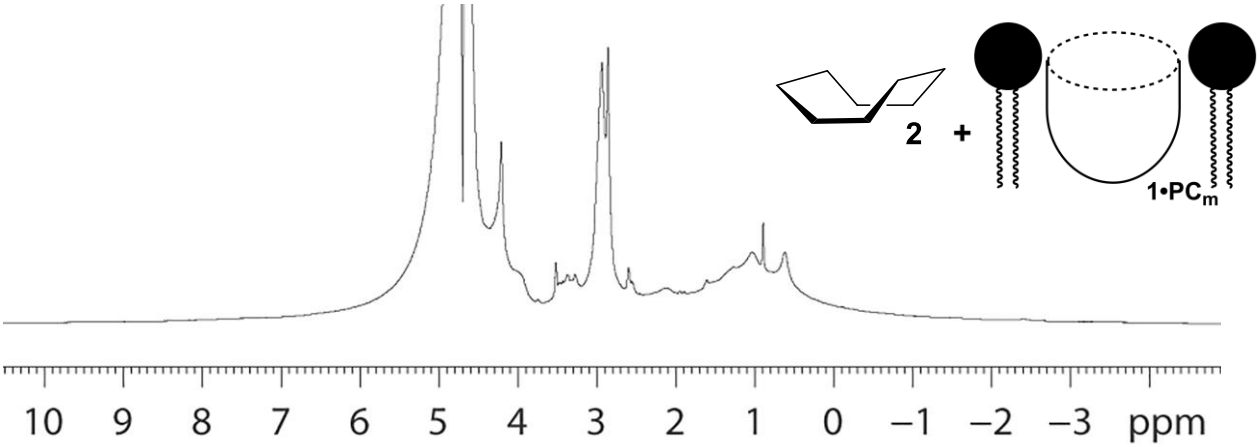

Figure S-26. T2-filtered ^{1}H NMR spectrum of the **1•2** cavitand-cyclooctane complex in DMPC:DHPC lipid micelles (599.88 MHz, 1 mM HEPES/D_2O, 298 K, [**1**] = [**2**] = 1.8 mM, ratio DMPC/DHPC = 3.2:1, 60 mg/mL total lipid concentration).

Guest 3

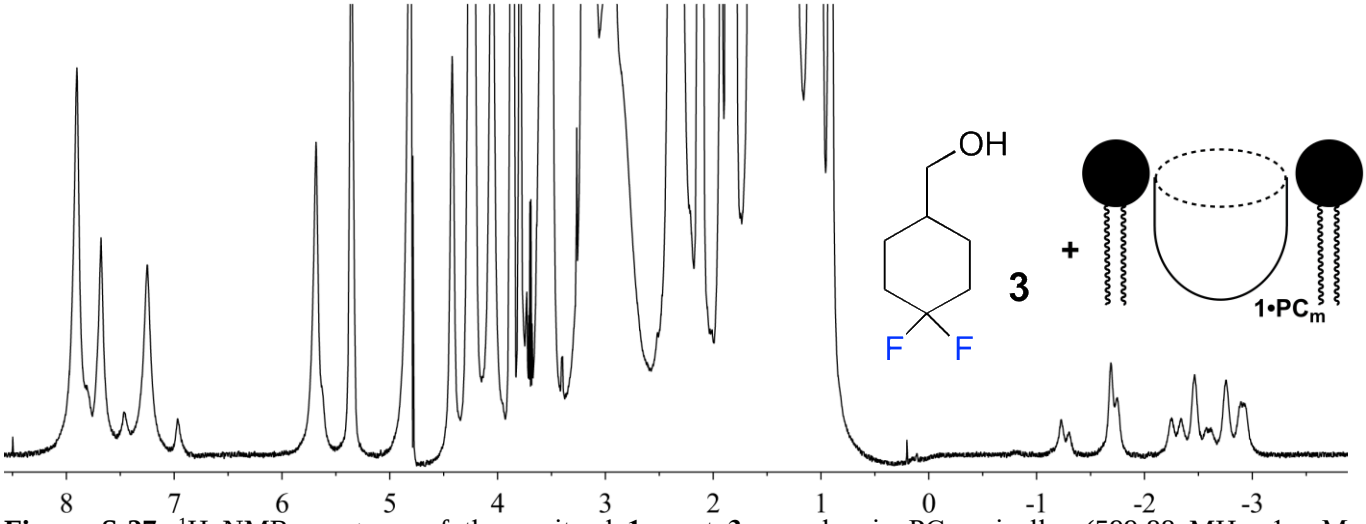

Figure S-27. ^{1}H NMR spectrum of the cavitand **1**•guest **3** complex in PC_m micelles (599.88 MHz, 1 mM HEPES/D_2O, 283 K, [**1**] = 5.8 mM, [**3**] = 39.5 mM, ratio DMPC/DHPC = 3.2:1, 60 mg/mL total lipid concentration).

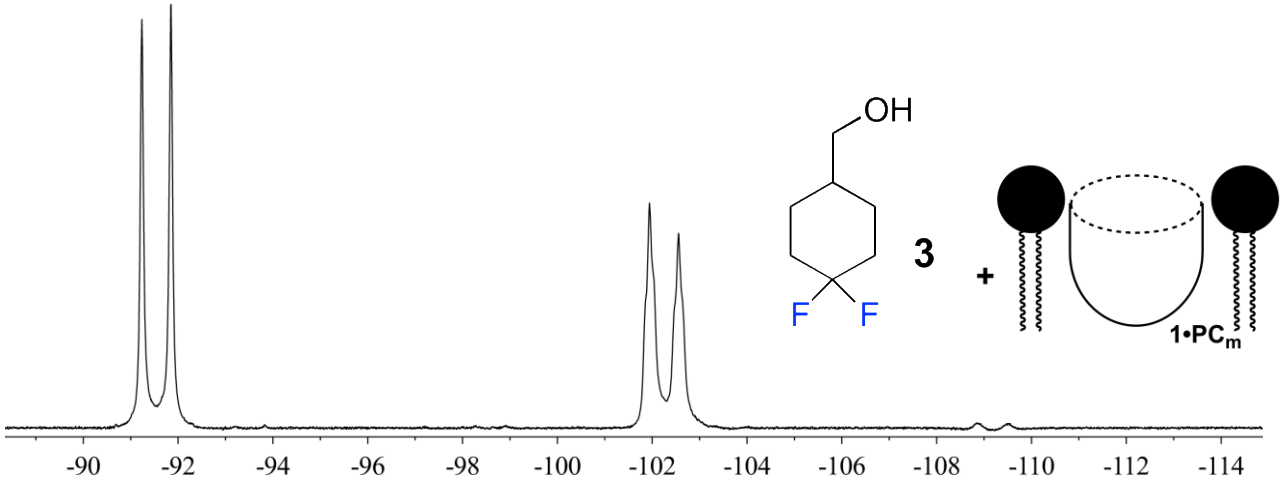

Figure S-28. ^{19}F NMR spectrum of the cavitand **1**•guest **3** complex in PC_m micelles (1 mM HEPES/D_2O, 376.50 MHz, 298 K, [**1**] = 5.8 mM, [**3**] = 39.5 mM, ratio DMPC/DHPC = 3.2:1, 60 mg/mL total lipid concentration).

Guest 4

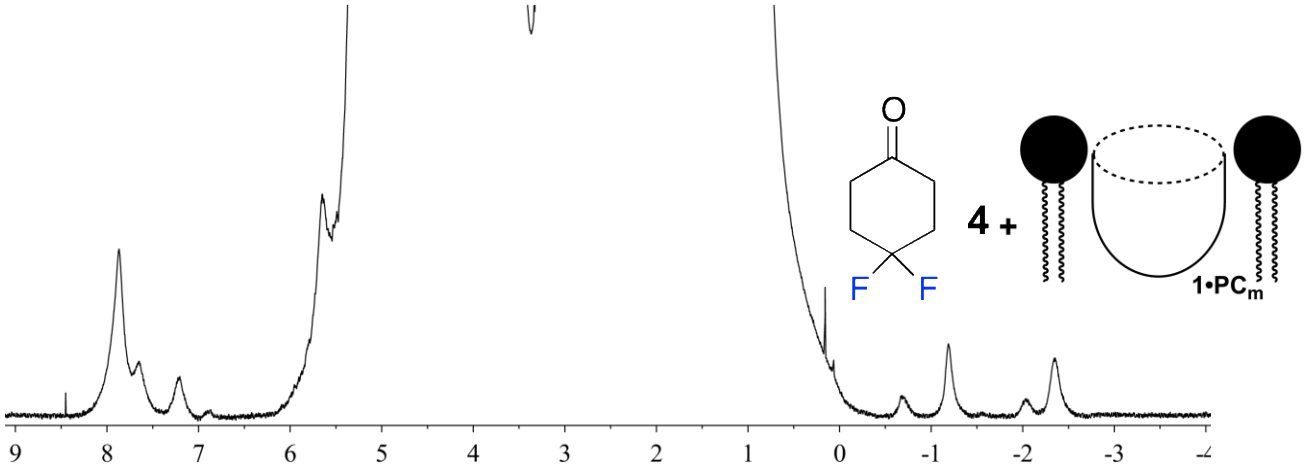

Figure S-29. ^{1}H NMR spectrum of the cavitand **1**•guest **4** complex in PC_m micelles (599.88 MHz, 1 mM HEPES/D_2O, 283 K, [**1**] = 5.8 mM, [**4**] = 39.5 mM, ratio DMPC/DHPC = 3.2:1, 60 mg/mL total lipid concentration).

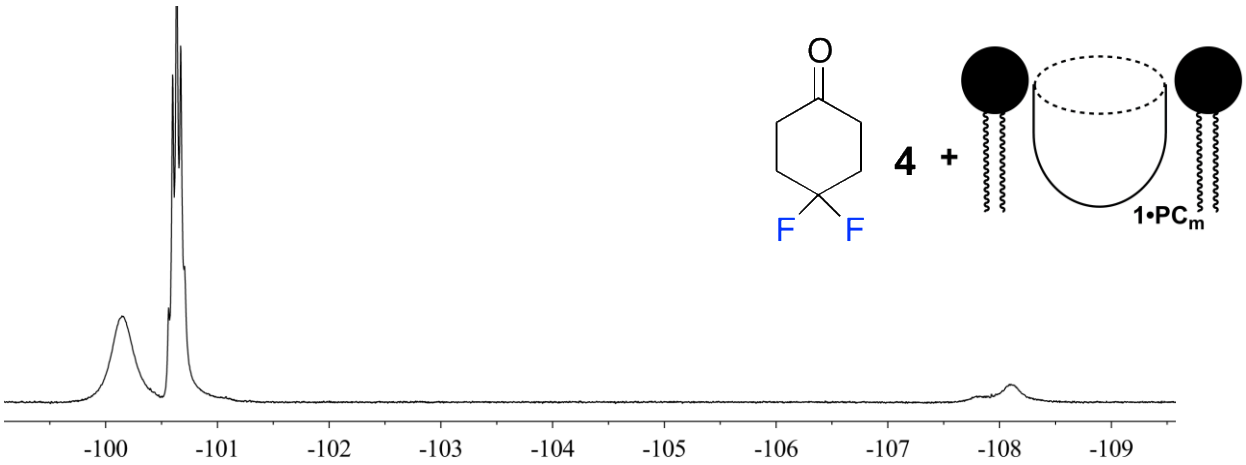

Figure S-30. ^{19}F NMR spectrum of the cavitand **1**•guest **4** complex in PC_m micelles **(**1 mM HEPES/D_2O, 376.50 MHz, 298 K, [**1**] = 5.8 mM, [**4**] = 39.5 mM, ratio DMPC/DHPC = 3.2:1, 60 mg/mL total lipid concentration);

Guest 6

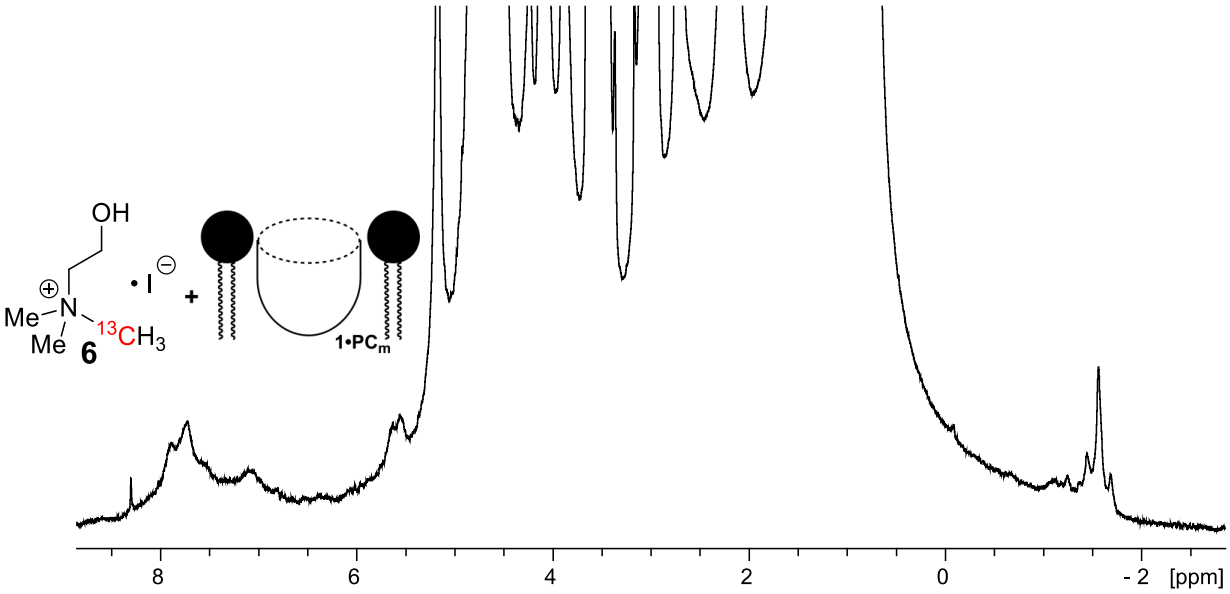

Figure S-31. ^{1}H NMR spectrum of the **1•6** cavitand-choline **6** complex in DMPC:DHPC lipid micelles (599.88 MHz, 1 mM HEPES/D_2O, 283 K, [**1**] = 5.8 mM, [**6**] = 16.0 mM, ratio DMPC/DHPC = 3.2:1, 60 mg/mL total lipid concentration).

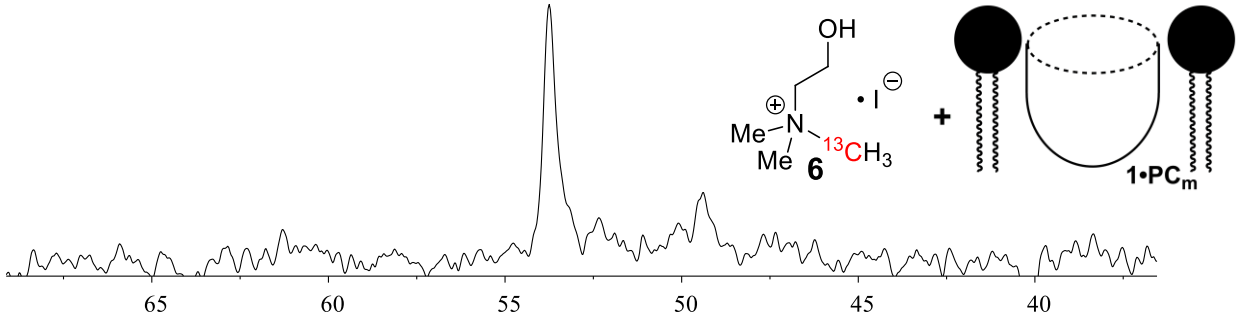

Figure S-32. ^{13}C NMR spectrum of the **1•6** cavitand-choline **6** complex in DMPC:DHPC lipid micelles (100.61 MHz, 1 mM HEPES/D_2O, 283 K, [**1**] = 5.8 mM, [**6**] = 16.0 mM, ratio DMPC/DHPC = 3.2:1, 60 mg/mL total lipid concentration).

Guest 7

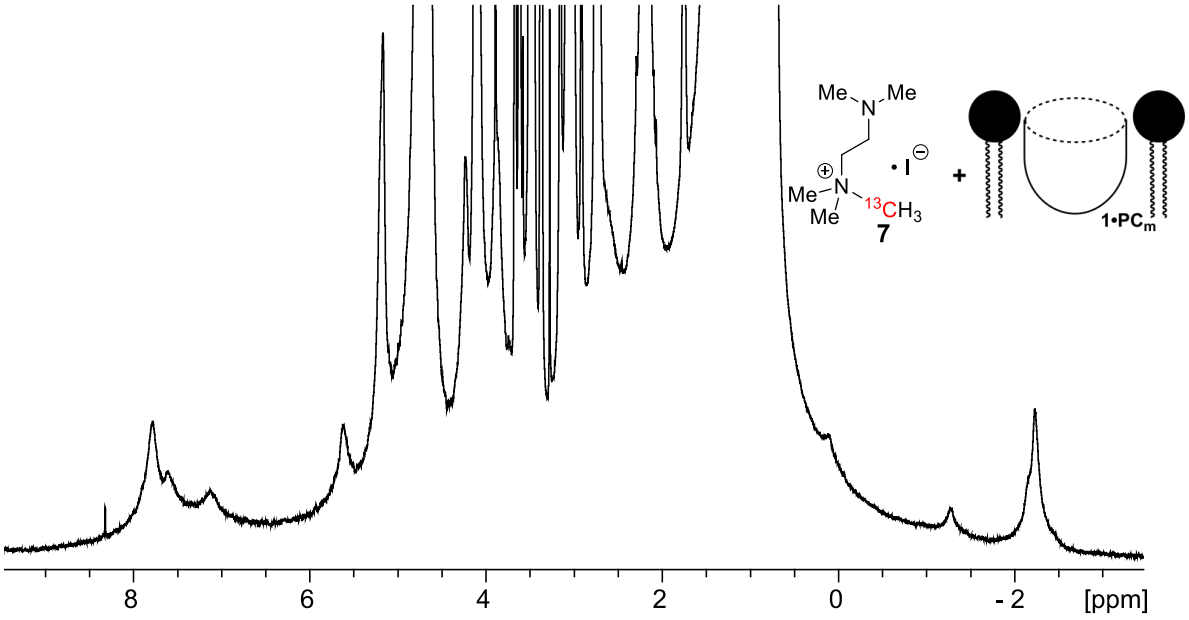

Figure S-33. ^{1}H NMR spectrum of the **1•7** cavitand-guest **7** complex in DMPC:DHPC lipid micelles (599.88 MHz, 1 mM HEPES/D_2O, 283 K, [**1**] = 5.8 mM, [**7**] = 16 mM, ratio DMPC/DHPC = 3.2:1, 60 mg/mL total lipid concentration).

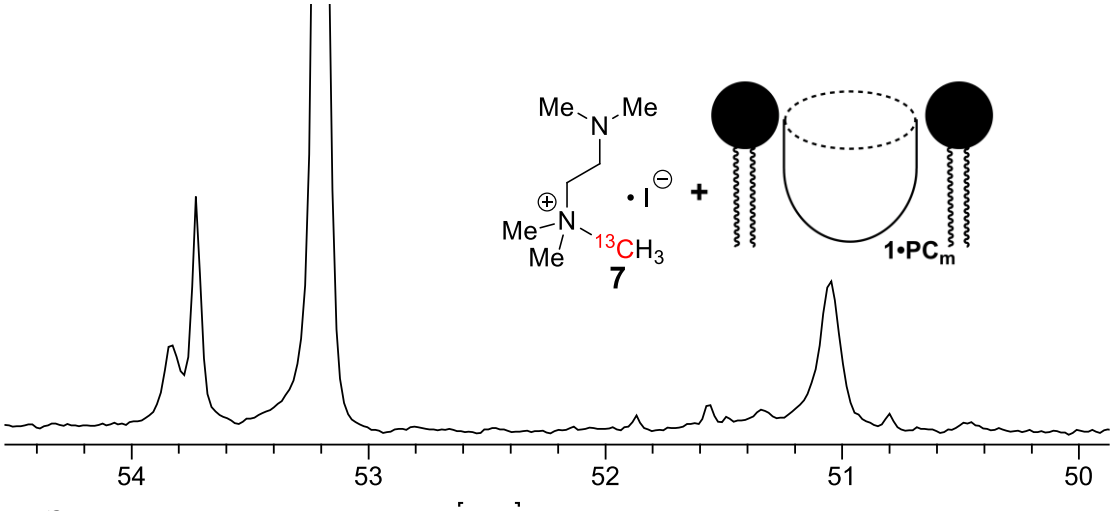

Figure S-34. ^{13}C NMR spectrum of the **1•7** cavitand-guest **7** complex in DMPC:DHPC lipid micelles (100.61 MHz, 1 mM HEPES/D_2O, 283 K, [**1**] = 5.8 mM, [**7**] = 16 mM, ratio DMPC/DHPC = 3.2:1, 60 mg/mL total lipid concentration).

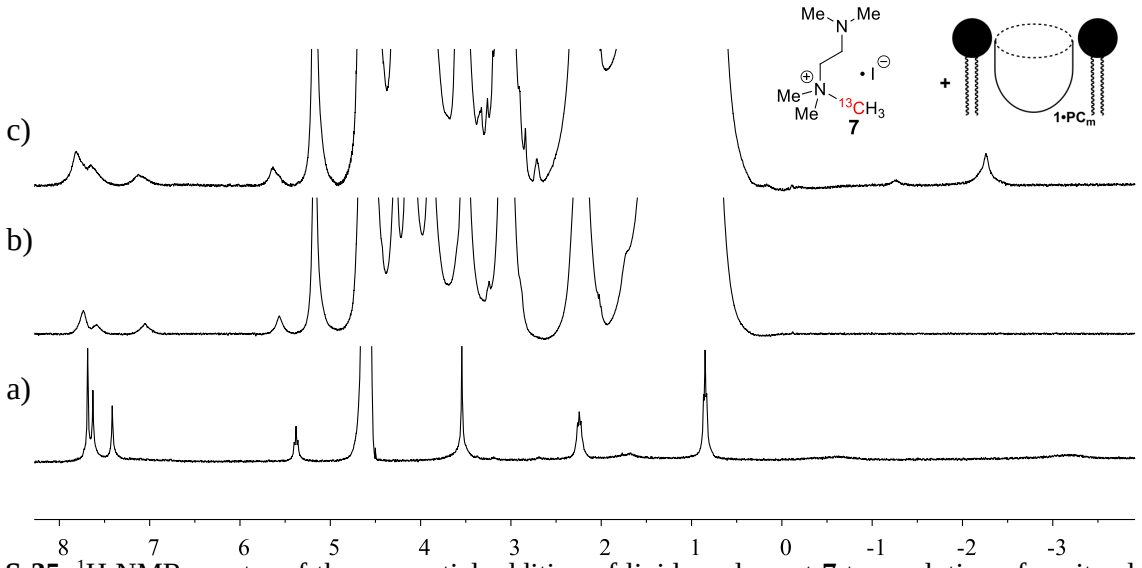

Figure S-35. ^{1}H NMR spectra of the sequential addition of lipids and guest **7** to a solution of cavitand **1** (400.13 MHz, 1 mM HEPES/D_2O, 298 K). a) 1.8 mM of cavitand **1**; b) 1.8 mM of cavitand **1** + DMPC/DHPC lipids, ratio DMPC/DHPC = 3.2:1, 60 mg/mL total lipid concentration; c) 1.8 mM of cavitand **1** + DMPC/DHPC lipids =2.2 mM guest **7**.

Guest 8

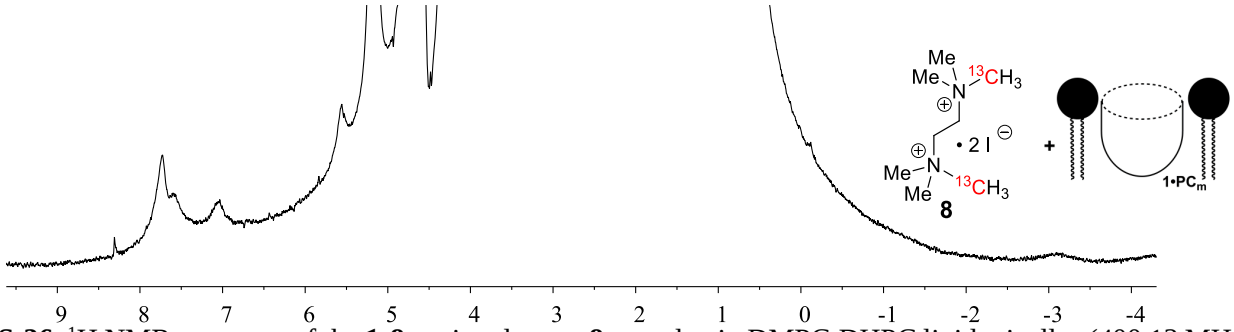

Figure S-36. ^{1}H NMR spectrum of the **1•8** cavitand-guest **8** complex in DMPC:DHPC lipid micelles (400.13 MHz, 1 mM HEPES/D_2O, 298 K, [**1**] = 1.8 mM, [**8**] = 5.4 mM, ratio DMPC/DHPC = 3.2:1, 60 mg/mL total lipid concentration).

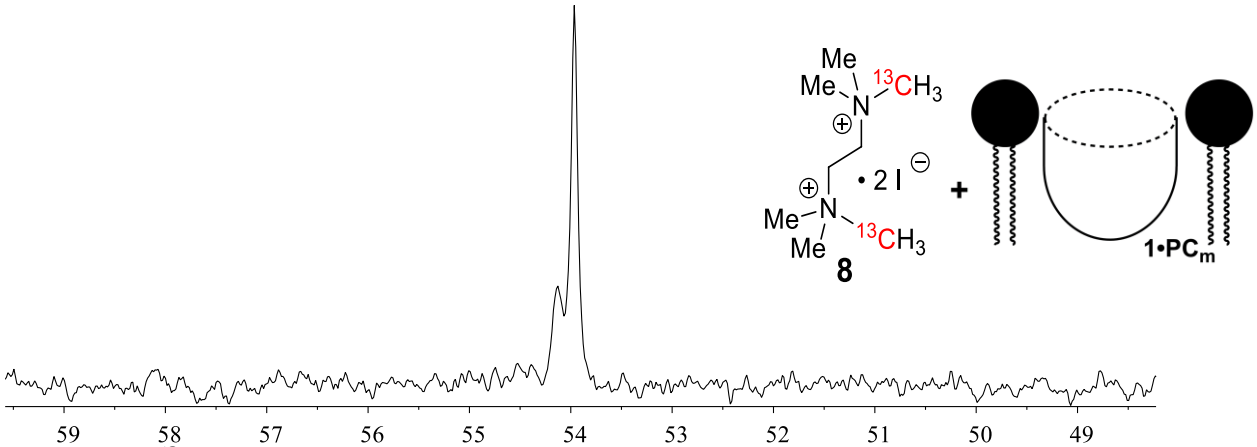

Figure S-37. ^{13}C NMR spectrum of the **1•8** cavitand-guest **8** complex in DMPC:DHPC lipid micelles (100.61 MHz, 1 mM HEPES/D_2O, 298 K, [**1**] = 1.8 mM, [**8**] = 5.4 mM, ratio DMPC/DHPC = 3.2:1, 60 mg/mL total lipid concentration).

4. Fitting model for EXSY Experiments

A standard two-site exchange model is used to analyze the EXSY data. In this model, the guest can exchange between a free and bound state, A and B, respectively:

$$A \underset{k_b}{\overset{k_f}{\rightleftharpoons}} B$$

k_b is the exchange constant from B to A, while k_f is the exchange constant for A to B. At equilibrium, the forward and reverse exchange rates are equal. Therefore $k_b[B] = k_f[A]$, or in terms of the equilibrium constant:

$$\frac{[B]}{[A]} = \frac{k_f}{k_b} = K_{eq},$$

During the mixing time of the EXSY experiment, the concentration of A can change in three ways: first, A can become bound, decreasing its contribution to the signal intensity over the mixing time; second, A can relax due to T_1, also decreasing its intensity; third, a bound ligand B can be released, becoming A and adding to its signal intensity. This can be described by the following first-order differential equation:

$$\frac{d[A]}{dt} = -k_f[A] - \frac{[A]}{T_{1A}} + k_b[B]$$

The signal from B varies in a similar way, giving

$$\frac{d[B]}{dt} = -k_b[B] - \frac{[B]}{T_{1B}} + k_f[A]$$

Each exchange spectrum contains two diagonal peaks, AA and BB, and two crosspeaks, AB and BA; the first letter refers to the frequency in f_1 of the EXSY spectrum, while the second gives the frequency in f_2 (hence AB would be the cross peak at $\{\nu_A, \nu_B\}$). The above set of coupled, first-order, linear differential equations can be solved using standard methods subject to the following initial conditions at the start of the EXSY mixing time:

AA and AB: $[A(t=0)] = A_0$, $[B(t=0)] = 0$

BB and BA: $[A(t=0)] = 0$, $[B(t=0)] = B_0$

giving the following expressions for the diagonal and cross peak intensities in terms of the EXSY mixing time (t):

$$AA(t) = A_0 e^{-t/T_1} \frac{k_b + e^{-(k_b+k_f)t} k_f}{k_b + k_f} \overset{\text{short time}}{\approx} A_0\left(1 - \tfrac{t}{T_1} - k_f t\right)$$

$$AB(t) = A_0 e^{-t/T_1} \frac{\left(1 - e^{-(k_b+k_f)t}\right) k_f}{k_b + k_f} \overset{\text{short time}}{\approx} A_0 k_f t$$

$$BB(t) = B_0 e^{-t/T_1} \frac{e^{-(k_b+k_f)t} k_b + k_f}{k_b + k_f} \overset{\text{short time}}{\approx} B_0\left(1 - \tfrac{t}{T_1} - k_b t\right)$$

$$BA(t) = B_0 e^{-t/T_1} \frac{\left(1 - e^{-(k_b+k_f)t}\right) k_b}{k_b + k_f} \overset{\text{short time}}{\approx} B_0 k_b t$$

where it has been assumed that $T_{1A} = T_{1B}$. The initial rate (short time) solutions are shown to the right. By extracting one-dimensional slices showing the greatest peak intensity from 2D spectra recorded with different mixing times, it is possible to fit the above set of equations and determine both k_b and k_f.

5. 2D Exchange NMR Spectra in Water and in Lipid Micelles

Guest 3

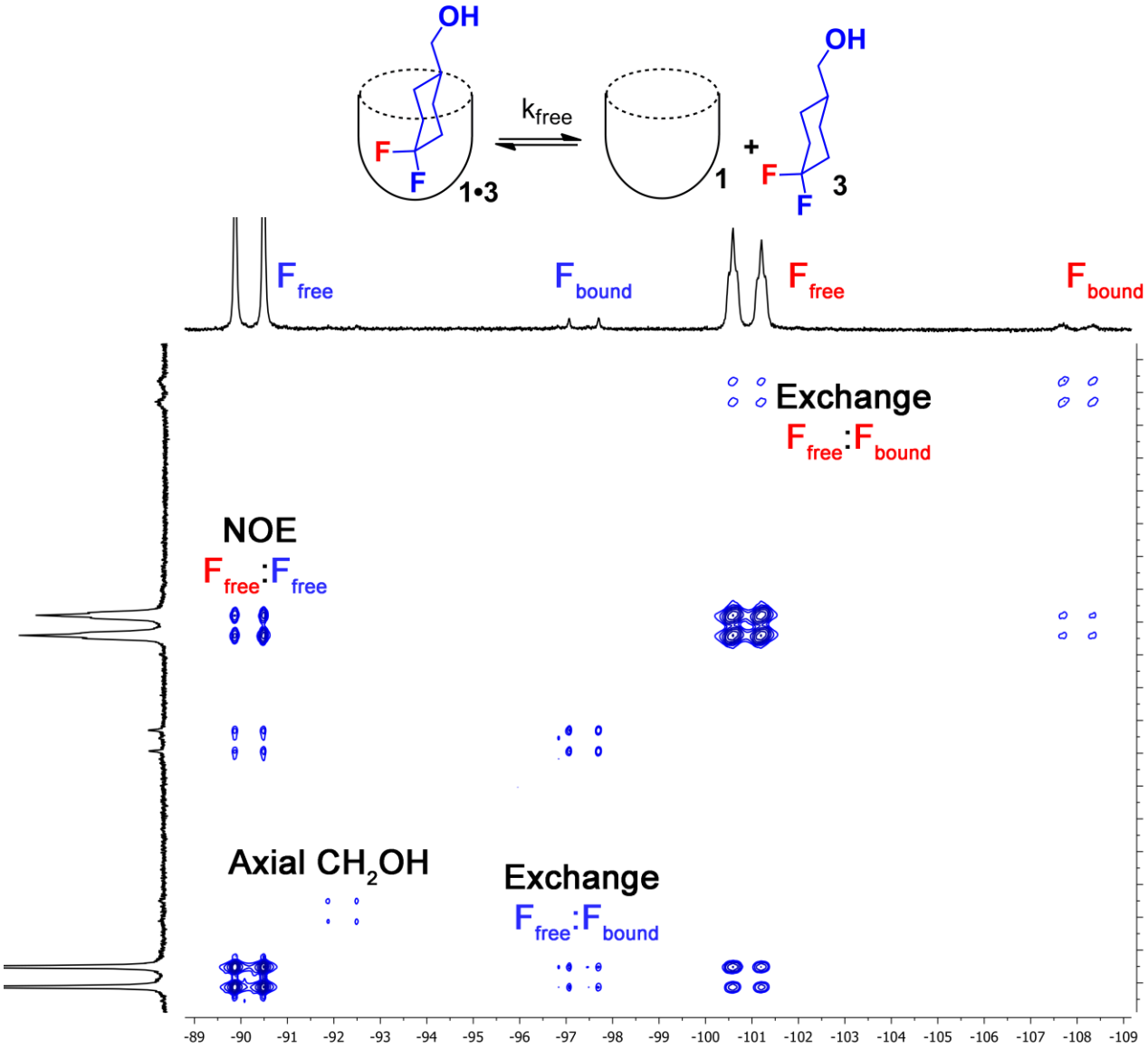

Figure S-38. Full ^{19}F EXSY spectrum of the cavitand **1**•guest **3** complex in pure D_2O with peak assignments (D_2O, 150.84 MHz, 298 K, mixing time = 150 ms, [**1**] = 5.8 mM, [**3**] = 39.5 mM)

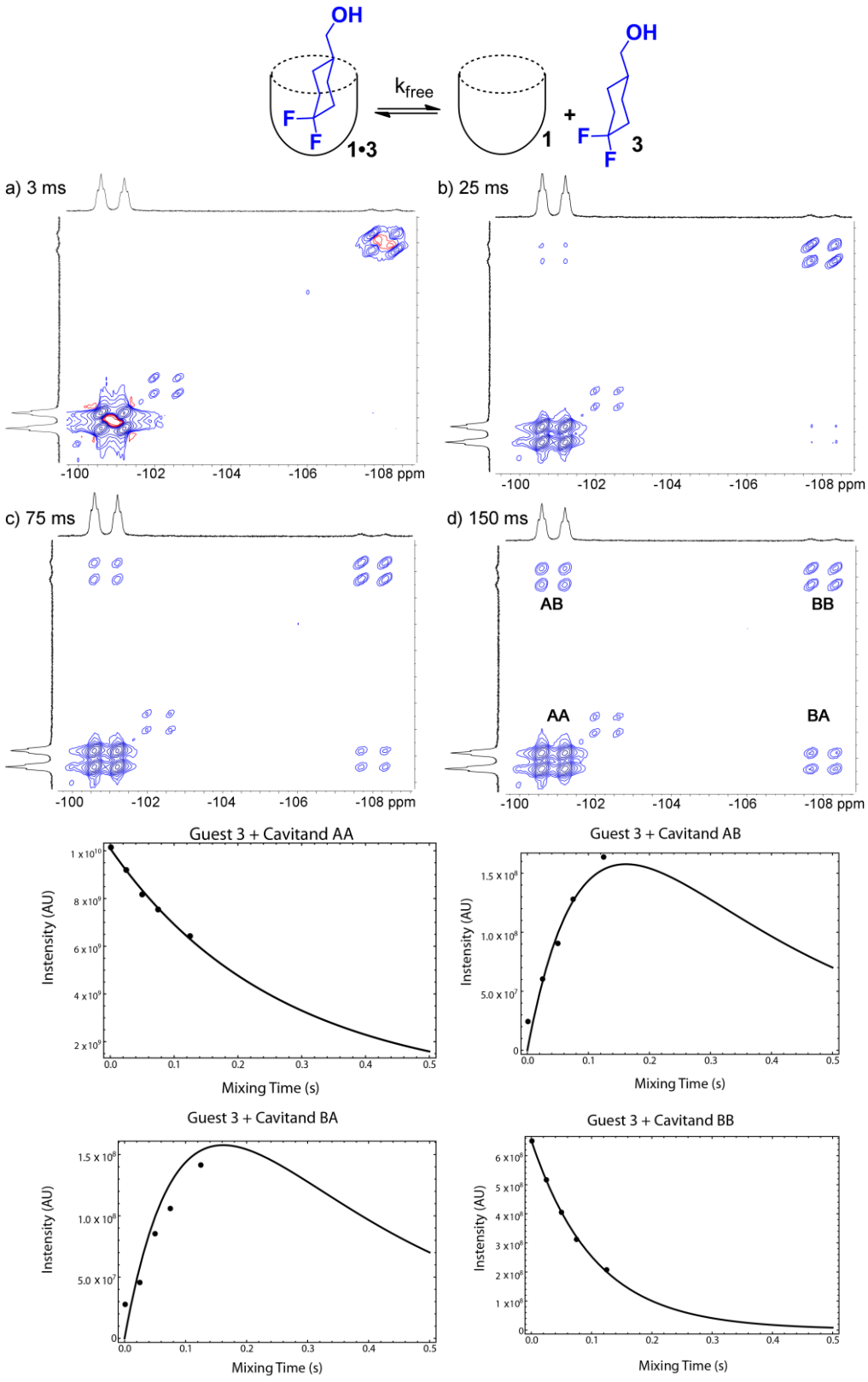

Figure S-39. Representative ^{19}F EXSY spectra of the cavitand **1**•guest **3** complex in pure D_2O with varying mixing times (D_2O, 376.50 MHz, 298 K, [**1**] = 5.8 mM, [**3**] = 39.5 mM); fitted plots of peak intensity correlated with mixing time for each diagonal and crosspeak used to calculate the exchange rate.

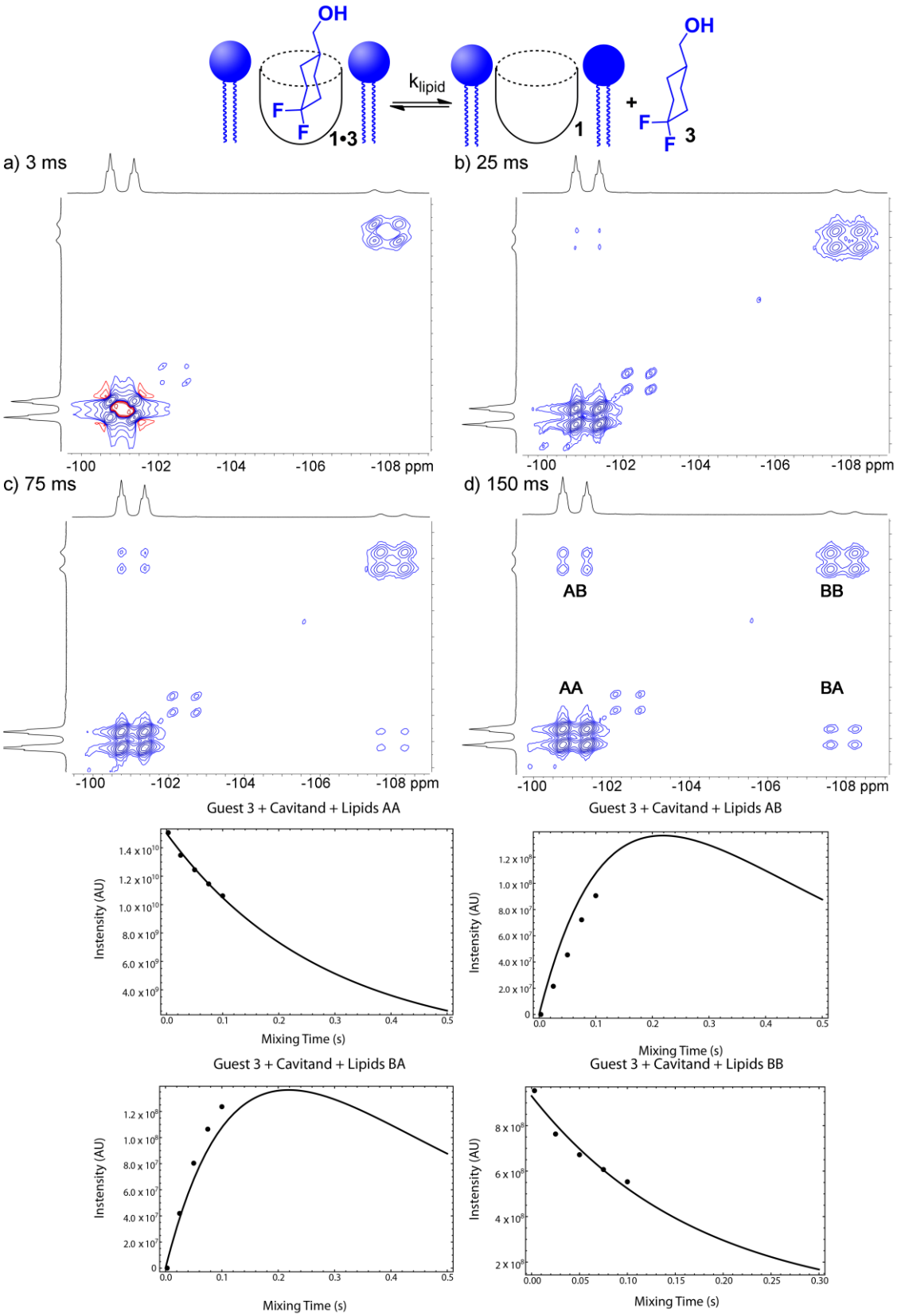

Figure S-40. Representative ^{19}F EXSY spectra of the cavitand **1**•guest **3** complex in the PC_m micelles with varying mixing times **(**1 mM HEPES/D_2O, 376.50 MHz, 298 K, [**1**] = 5.8 mM, [**3**] = 39.5 mM, ratio DMPC/DHPC = 3.2:1, 60 mg/mL total lipid concentration); fitted plots of peak intensity correlated with mixing time for each diagonal and crosspeak used to calculate the exchange rate.

Guest 4

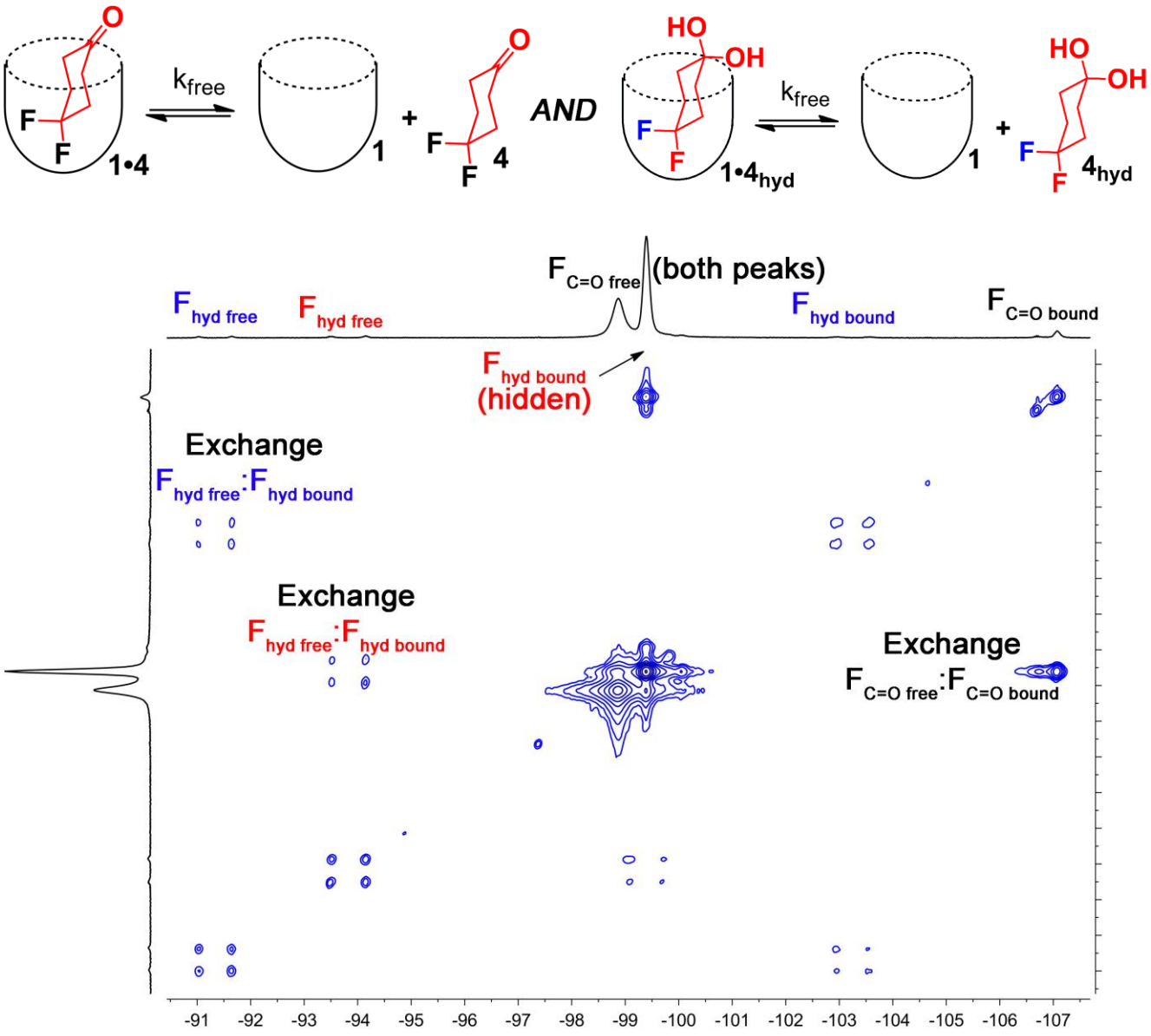

Figure S-41. Full ^{19}F EXSY spectrum of the cavitand **1**•guest **4** complex in pure D_2O with peak assignments (D_2O, 150.84 MHz, 298 K, mixing time = 150 ms, [**1**] = 5.8 mM, [**4**] = 39.5 mM).

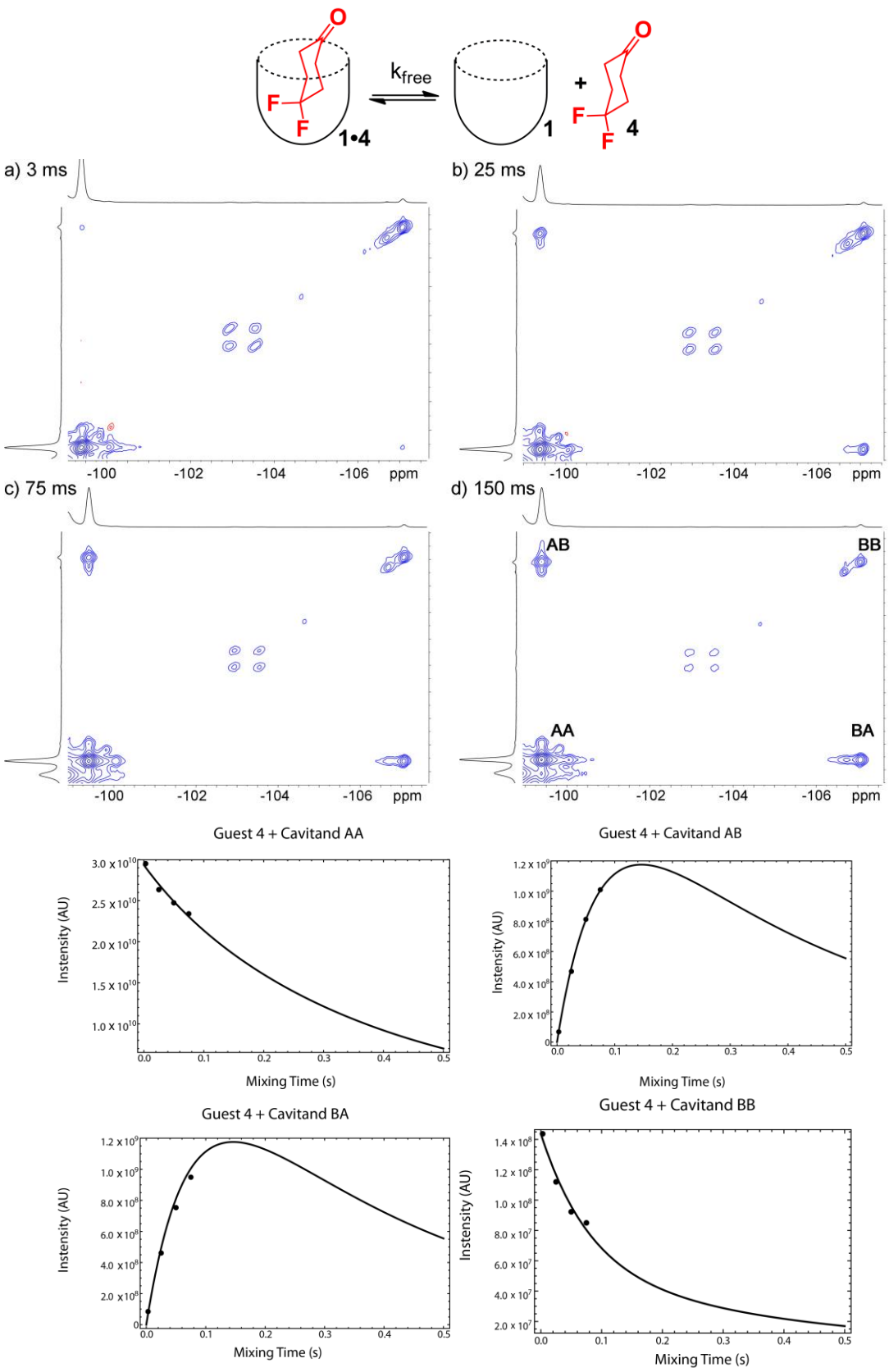

Figure S-42. Representative ^{19}F EXSY spectra of the cavitand **1**•guest **4** complex in pure D_2O with varying mixing times (D_2O, 376.50 MHz, 298 K, [**1**] = 5.8 mM, [**4**] = 39.5 mM); fitted plots of peak intensity correlated with mixing time for each diagonal and crosspeak used to calculate the exchange rate.

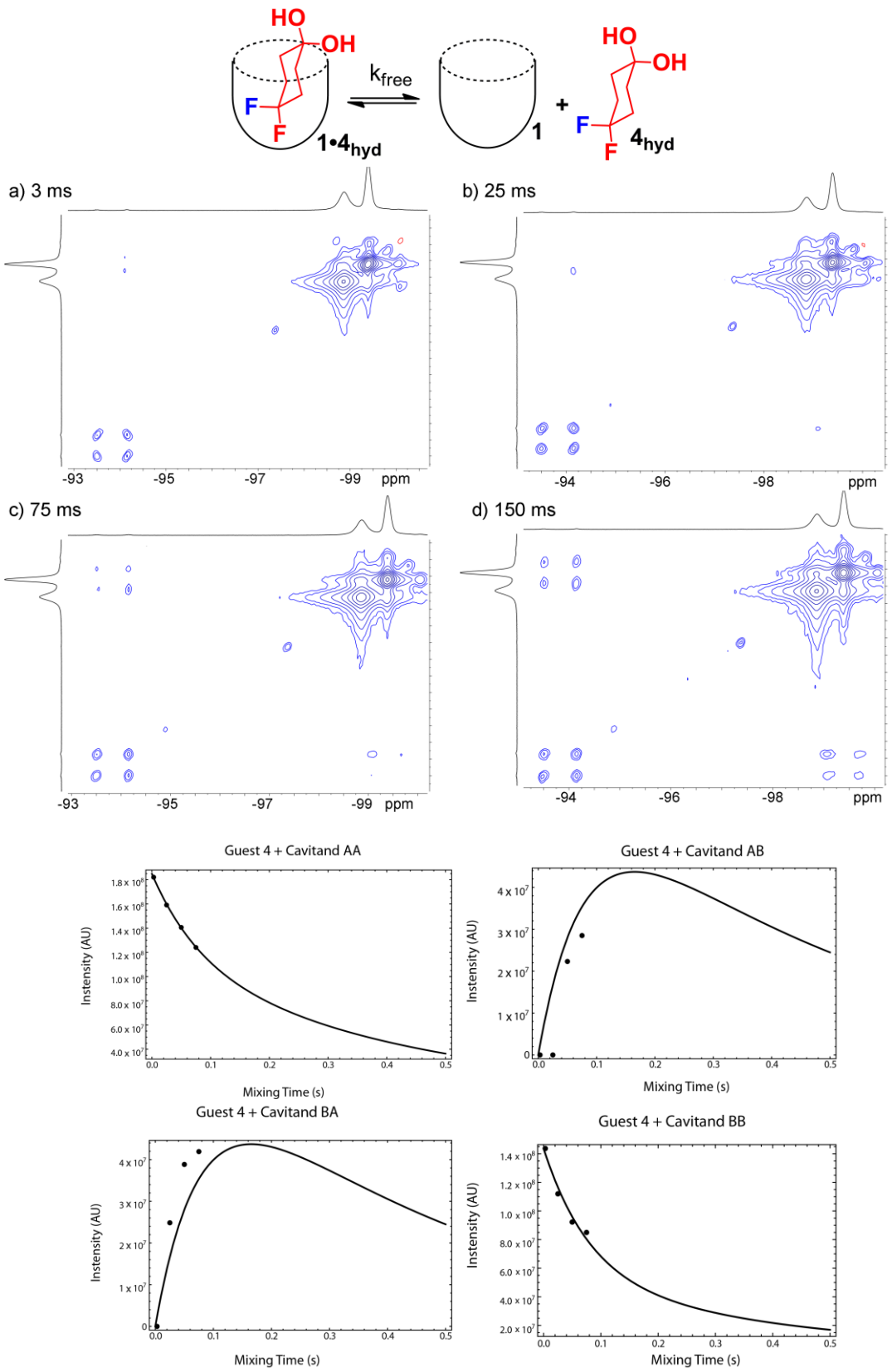

Figure S-43. Representative ^{19}F EXSY spectra of the cavitand **1**•guest **4** complex in pure D_2O with varying mixing times (D_2O, 376.50 MHz, 298 K, [**1**] = 5.8 mM, [**4**] = 39.5 mM) illustrating the exchange peaks of the hydrate; fitted plots of peak intensity correlated with mixing time for each diagonal and crosspeak used to calculate the exchange rate.

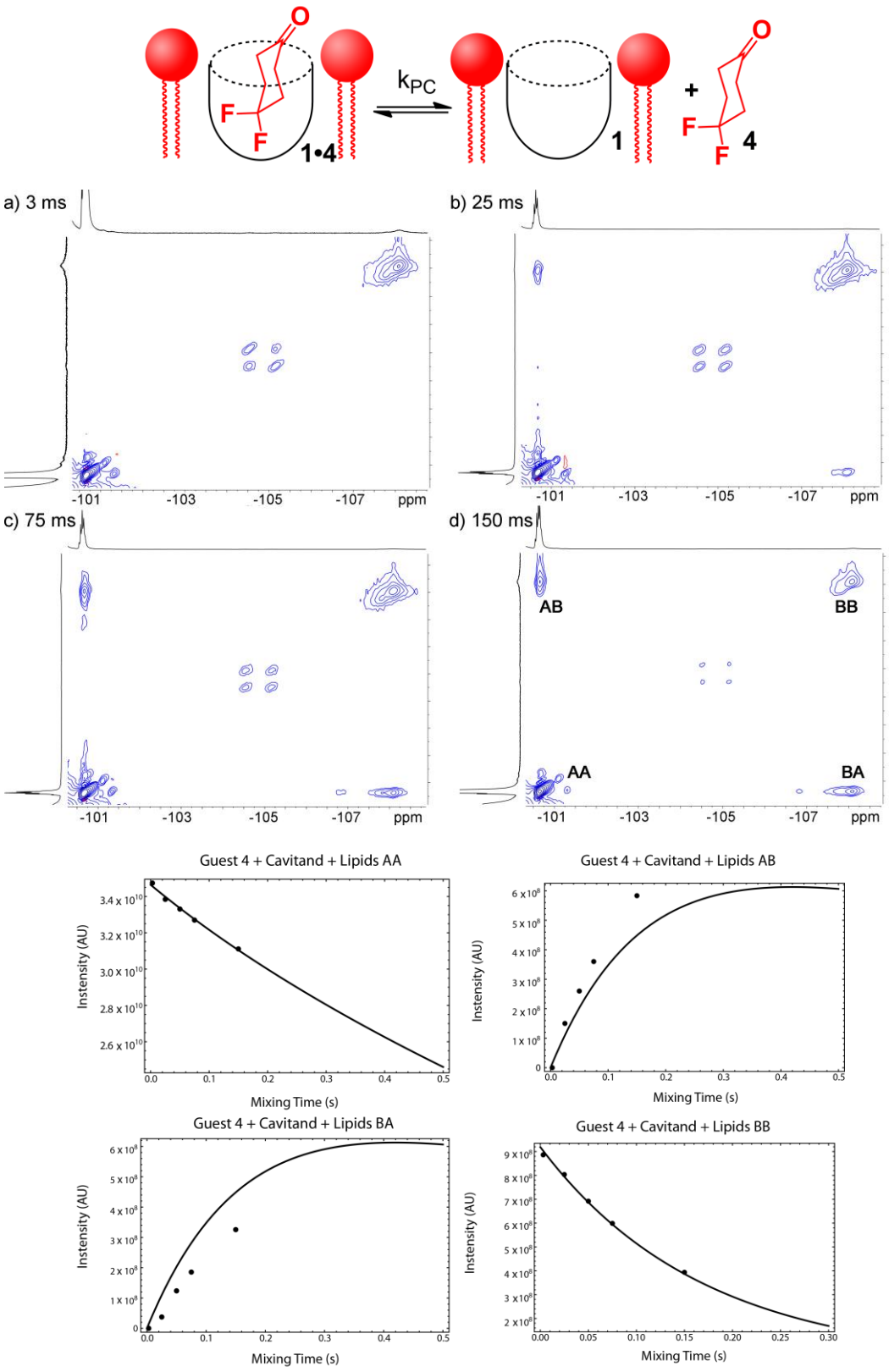

Figure S-44. Representative ^{19}F EXSY spectra of the cavitand **1**•guest **4** complex in the PC_m micelles with varying mixing times (1 mM HEPES/D_2O, 376.50 MHz, 298 K, [**1**] = 5.8 mM, [**4**] = 39.5 mM, ratio DMPC/DHPC = 3.2:1, 60 mg/mL total lipid concentration); fitted plots of peak intensity correlated with mixing time for each diagonal and crosspeak used to calculate the exchange rate.

Guest 6

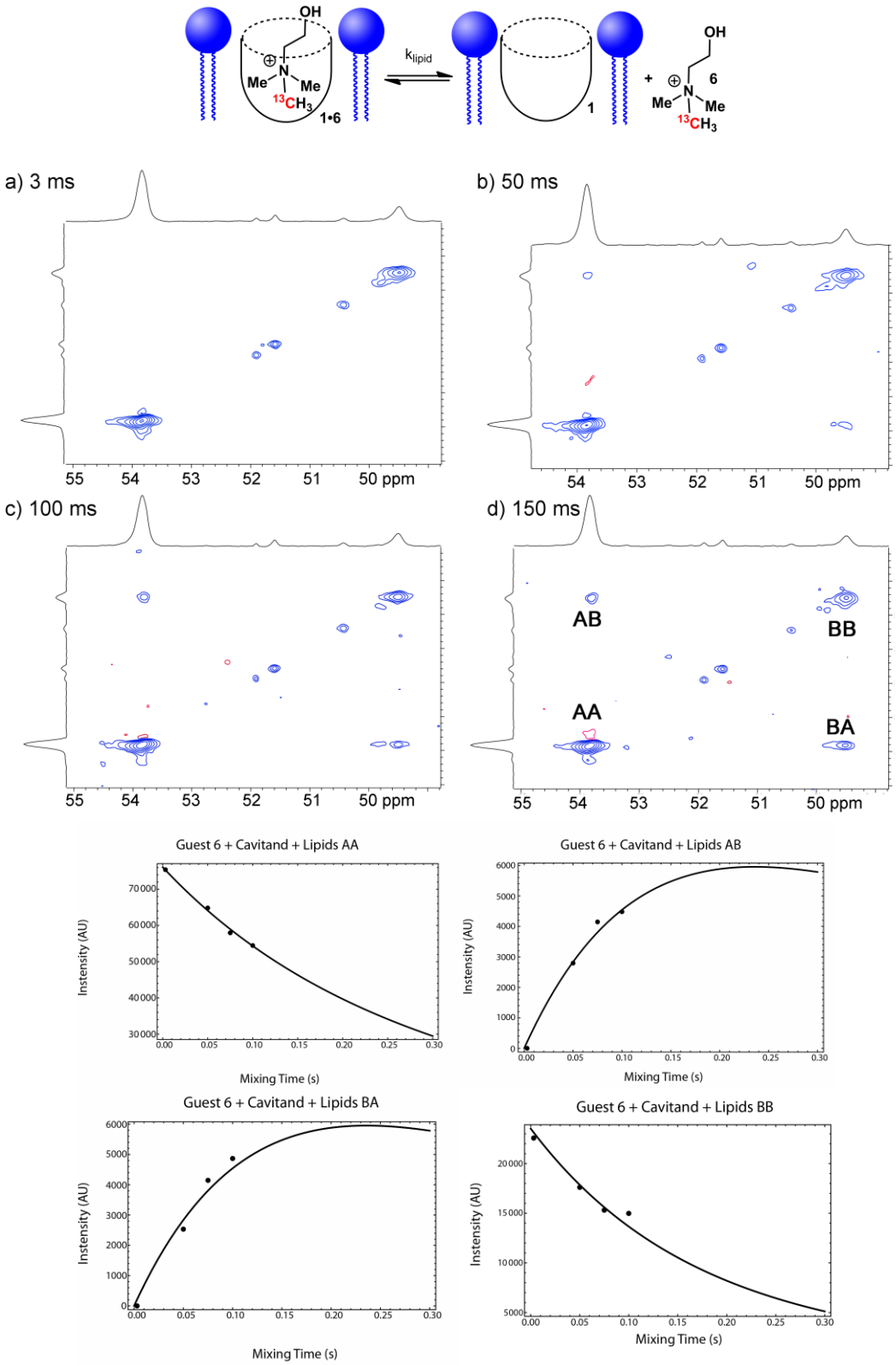

Figure S-45. Representative ^{13}C EXSY spectra of the cavitand **1**•guest **6** complex in the PC_m micelles with varying mixing times (1 mM HEPES/D_2O, 150.84 MHz, 298 K, [**1**] = 5.8 mM, [**6**] = 16 mM, ratio DMPC/DHPC = 3.2:1, 60 mg/mL total lipid concentration); fitted plots of peak intensity correlated with mixing time for each diagonal and crosspeak used to calculate the exchange rate.

Guest 7

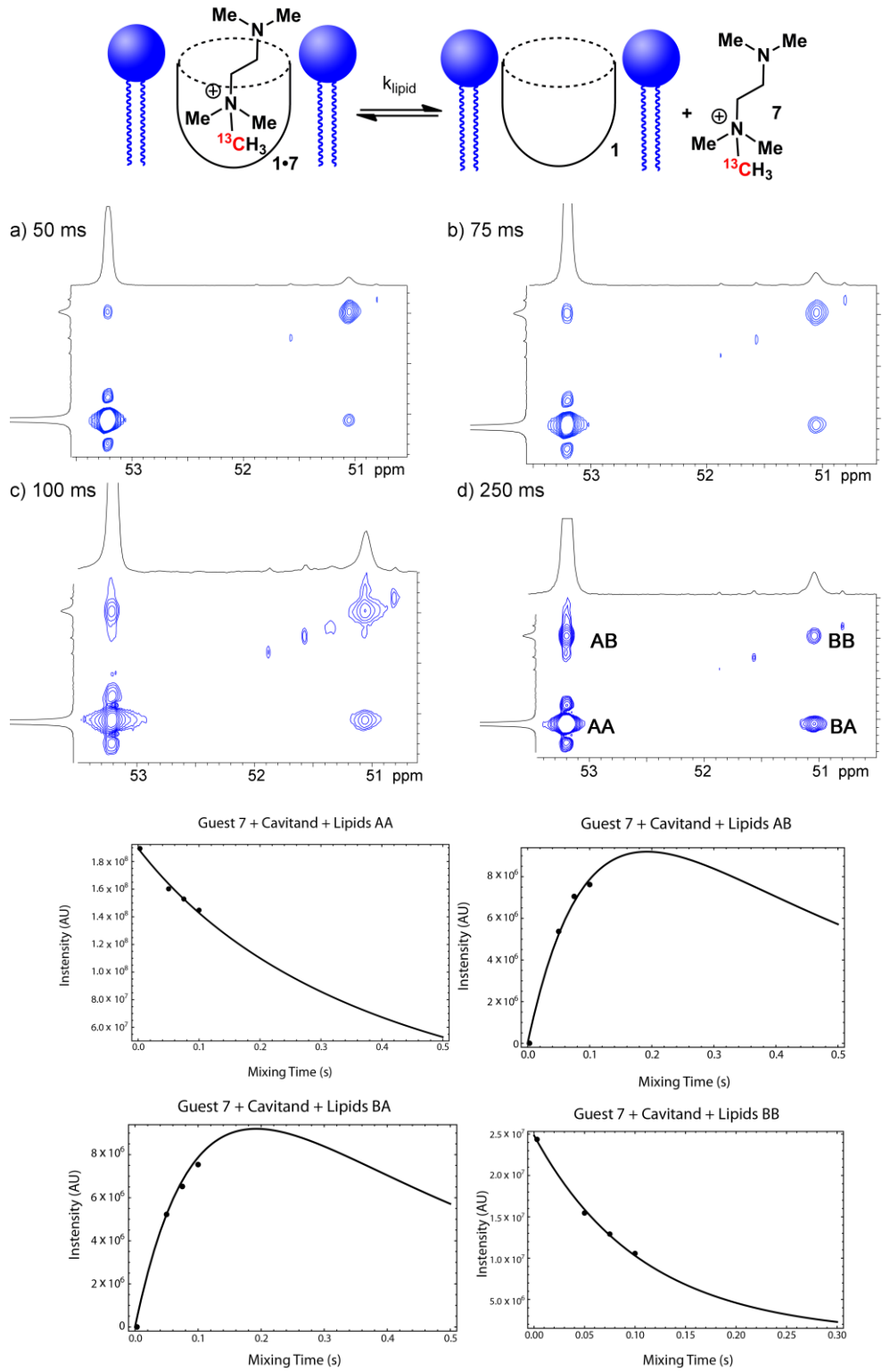

Figure S-46. Representative ^{13}C EXSY spectra of the cavitand **1**•guest **7** complex in the PC_m micelles with varying mixing times (1 mM HEPES/D_2O, 150.84 MHz, 298 K, [**1**] = 5.8 mM, [**7**] = 16 mM, ratio DMPC/DHPC = 3.2:1, 60 mg/mL total lipid concentration); fitted plots of peak intensity correlated with mixing time for each diagonal and crosspeak used to calculate the exchange rate.

6. NMR Spectra in Magnetically Ordered DMPC/DHPC Bicelles

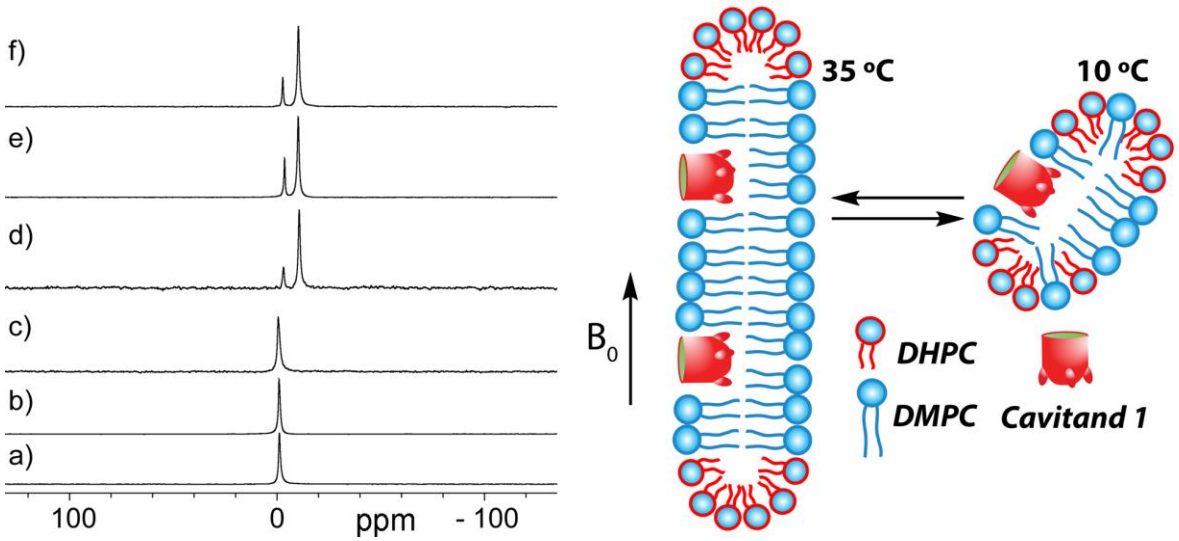

Figure S-47. Temperature dependence of the lipid aggregate. ^{31}P NMR spectra of the DMPC/DHPC aggregates a) alone, 283 K; b) + 5 mM **1**, 283 K; c) + 5 mM **1** + 7 mM guest **5**, 283 K; d) alone, 303 K; e) + 5 mM 1, 303 K; f) + 5 mM **1** + 7 mM guest **5**, 303 K. Ratio DMPC/DHPC = 3.2:1, 150 mg/mL total lipid concentration, 162.07 MHz, 2.5 mM HEPES/D_2O.

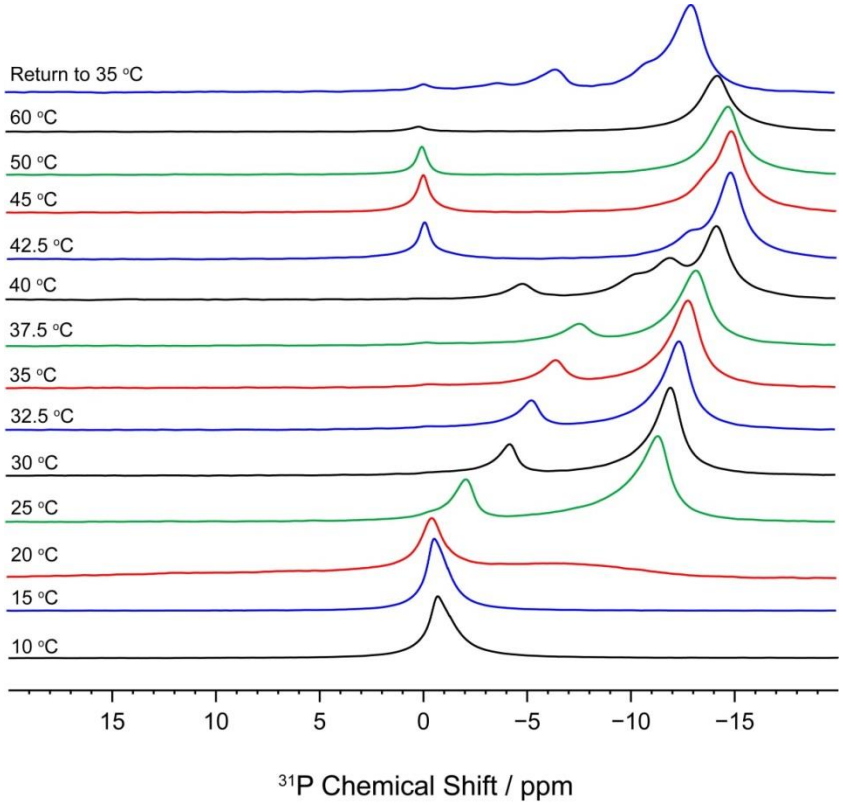

Figure S-48. Temperature-dependent ^{31}P spectra of DMPC/DHPC bicelles. The two peaks indicative of bicelle formation display maximum splitting at 35 °C, the temperature at which all future experiments were performed, unless otherwise indicated. Low temperatures display a single peak at 0 ppm, indicative of micelle formation. Ratio DMPC/DHPC = 3.2:1, 150 mg/mL total lipid concentration, 162.07 MHz, 2.5 mM HEPES/D_2O.

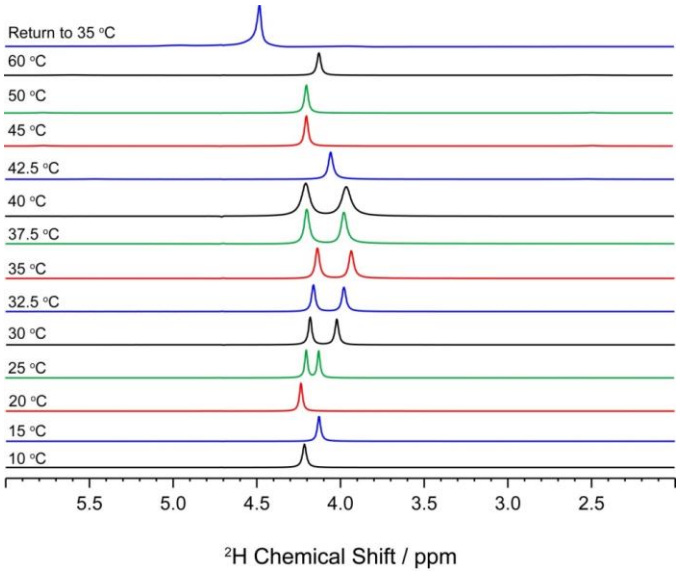

Figure S-49. Temperature-dependent ^{2}H spectra of DMPC/DHPC bicelles. The two peaks indicative of bicelle formation display maximum splitting at 35 °C, the temperature at which all future experiments were performed, unless otherwise indicated. Low temperatures display a single resonance, indicative of micelle formation. Ratio DMPC/DHPC = 3.2:1, 150 mg/mL total lipid concentration, 92.09 MHz, 2.5 mM HEPES/D_2O.

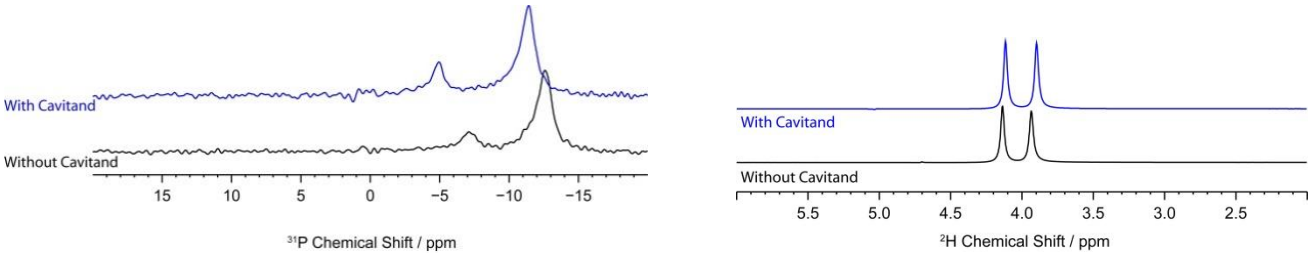

Figure S-50. ^{31}P and ^{2}H spectra of bicelles with and without cavitand added. Ratio DMPC/DHPC = 3.2:1, 150 mg/mL total lipid concentration, 162.07/ 92.09 MHz, 2.5 mM HEPES/D_2O.

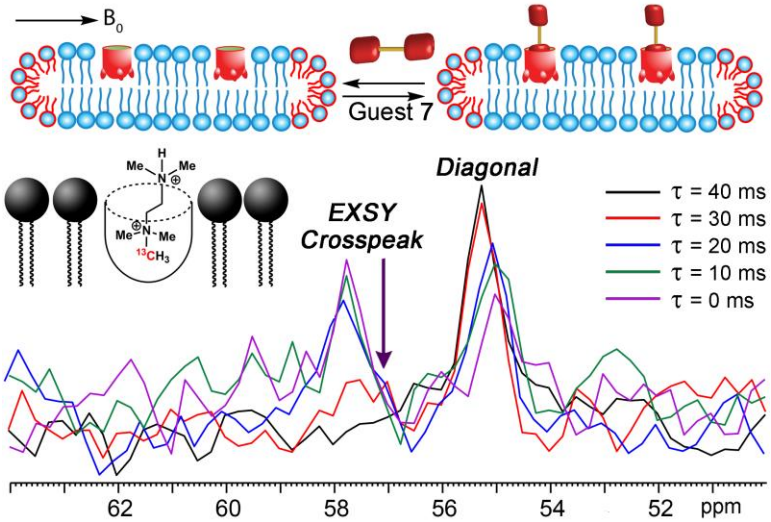

Figure S-51. In/out exchange of guest **7** in the magnetically ordered bicelle system PC_b. Extracted 1D slices of the 2D ^{13}C-^{13}C EXSY NMR spectra at mixing time τ = 0 ms - τ = 40 ms of **1•7•PC$_b$**; (2.5 mM HEPES/D_2O, 100.69 MHz, 298 K, [**1**] = 20 mM, [**7**] = 36 mM, ratio DMPC/DHPC = 3.2:1, 150 mg/mL total lipid concentration). Change in diagonal and crosspeak intensity shown. Slices extracted from F2, δ = 55 ppm.